MASTER'S THESIS

Micro-Damage Initiation and Evolution in GF/EP Cross-Ply Laminates

Hana Kriaa
2015

Master of Science (120 credits)
Materials Engineering

Luleå University of Technology
Department of Engineering Sciences and Mathematics

LULEÅ UNIVERSITY OF TECHNOLOGY

Microdamage initiation and evolution in GF/EP cross-ply laminates

MASTER THESIS

Hana Kriaa

Supervised by:

Prof. Janis Varna, Division of Materials Science

June 2015
Luleå University of Technology
Department of Engineering Science and Mathematics
Division of Materials Science

Preface

The master thesis work presented in this report titled 'Microdamage initiation and evolution in GF/EP cross-ply laminates'. It was carried out at the Division of Materials Sciences in the Department of Engineering Sciences and Mathematics of Luleå University of Technology during the second semester of 2015.

The successful completion of this thesis would not have been possible and could not have seen the light of day without the precious support of many persons.

I would like to thank everyone who has helped and supported me during the writing of my master thesis.

First of all I would like to express my gratitude to my supervisor Janis Varna who has shared with me his valuable knowledge, advice and time. I was so glad to discuss with him and I was proud to take from him valuable time despite his tight schedule, proud because I learnt directly from him. And without doubt, I thank him for his stand by me when I need help.

Moreover, I would like to give some special thanks to Doctor Hana Zrida , Hiba Ben Kahla, Liva Purpus and Andrejs Purpurs for their support. I never forget that they were welcoming my questions and helping me when I need support to make the work advance.

It is a pleasure to thank the Advanced Materials Science and Engineering program (AMASE) to gives me the opportunities to study in this amazing atmosphere.

Finally, I owe my deepest gratitude to my parents, my relatives, my brothers, my nephew and my fiance for their love, prayer, support, care and encouraging words that light my way and kindle my enthusiasm to bring out the best in me in all my academic endeavors.

Luleå University of Technology, June 2015

Hana Kriaa

Abstract

The desired characteristics of materials in modern industrial applications require high specific modulus and high specific strength for low specific weight. Composites structures are now the best candidates for this type of applications due to their high strength and stiffness to weight and they are widely used in different load carrying structures.

Under service loading, composite laminates, are subjected to complex combinations of thermal and mechanical loading, leading to micro-damage accumulation in the plies. Usually the first damage mode is intra-laminar cracking, the density of those cracks depends on layer orientation with respect to the load direction, temperature change, number of cycles in fatigue, laminate lay-up, ply thickness and, certainly, material toughness.

The effects of extreme environmental conditions on damage evolution and lifetime of composite laminates based on glass fiber epoxy are studied in this project experimentally and theoretically through the performing of quasi-static test and fatigue tensile test.

Keywords: glass fiber epoxy, damage evolution, quasi-static tensile test, fatigue tensile test**.**

Nomenclature

The symbols and abbreviations used in this thesis are listed here.

List of symbols:

l	Length of the fiber
d	Diameter of fiber
E_L	Longitudinal modulus
E_T	Transversal modulus
E	Young modulus
$\frac{E}{E_0}$	Normalized stiffness
G_{LT}	Longitudinal and transversal shear modulus
α_L	Thermal longitudinal expansion
α_T	Thermal transversal expansion
ν	Poison's ration
P_f	Probability of failure
ρ	Crack density
ρ_{max}	Maximum crack density
V	Volume of tested specimen
V_0	Reference volume
t	Thickness of the specimen
σ_T	Transverse stress
$\sigma_T^{90\ mech}$	Mechanical transverse stress
$\sigma_T^{90\ thermal}$	Thermal transverse stress

σ_0	Scale Weibull's parameter
n	Shape Weibull's parameter
ε	Strain
[Q]	Stiffness matrix
[T]	Transformation matrix
[A]	Extensional stiffness matrix
[B]	Coupling stiffness matrix
[D]	Bending stiffness matrix
N	Force per unit of width
M	The moment
K	The curvature
γ	Shear strain
σ_L σ_T σ_{LT}	Stresses in local system
ε_L ε_T ε_{LT}	Strains in local system
F_{max}	Maximum load of fatigue cycles
F_{min}	Minimum load of fatigue cycles
E_0	Initial Young modulus before performing fatigue test
R_R	Ramp rate
A	Area of the of tested specimen
N	Number of fatigue cycles

Abbreviations:

GF	Glass fiber
EP	Epoxy

CD	Crack density
CLT	Classical laminate theory

Table of content

Chapter 1:

Introduction

The laminated composite materials usage is increasing in all sorts of engineering applications like transportation vehicles, aviation industries, marine and aerospace this because of their mechanical and physical properties such as their high specific strength and stiffness.

A composite laminate is a structural plate consisting of multiple layers of fiber reinforcement covered in cured resin. The number of layers, the type of fiber (carbon, glass, or other), the fabric configuration (woven, stitched mat, uni-directional), the type of resin, and other factors may vary depending on the desired application. Raw materials (fiber, resin) in themselves are not useful as a structural member, but when combined together, the product takes on new properties that make them used in desirable structures. That is why high-level composite performance can be achieved only through correct selection of both the fiber reinforcements and the polymer matrix (resin) that binds them into a cohesive structural unit.

The aeronautics industry especially takes benefits from the performance of composites to develop the plane structure replacing metallic materials with the lighter ones.

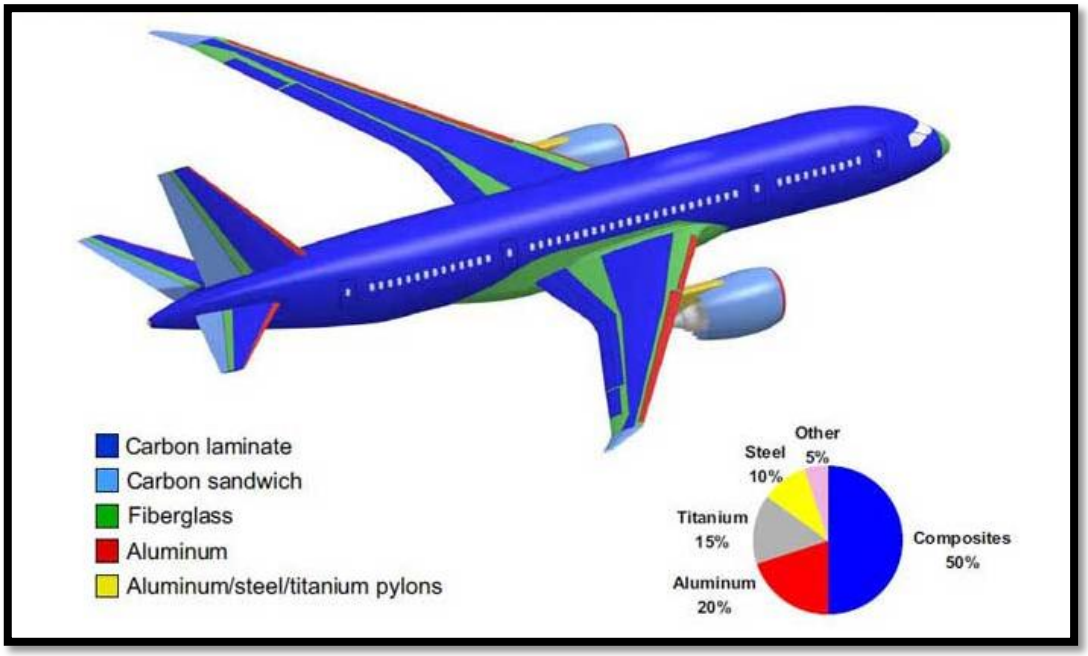

Figure 1.Boeing 787 Dreamliner commercial airplane. Source: The Boeing Company [1]

Due to the addition of fibers, the mechanical properties of the composite become complex and when subjected to a compression, tensile or fatigue tensile mechanical tests, the composites materials are susceptible to mechanical damages.

Chapter 2:

Literature review

1. Fiber reinforced composite materials

Fiber reinforced composite material consists of fibers with high strength and modulus incorporate or bonded to a matrix. A composite material is a material formed by the combination of at least two different phases where every phase has its mechanical, electrical chemical and physical properties. Combining together, the components give a composite material with better properties than each component separately. In contrast to metallic alloys, each material retains its separate chemical, physical, and mechanical properties.

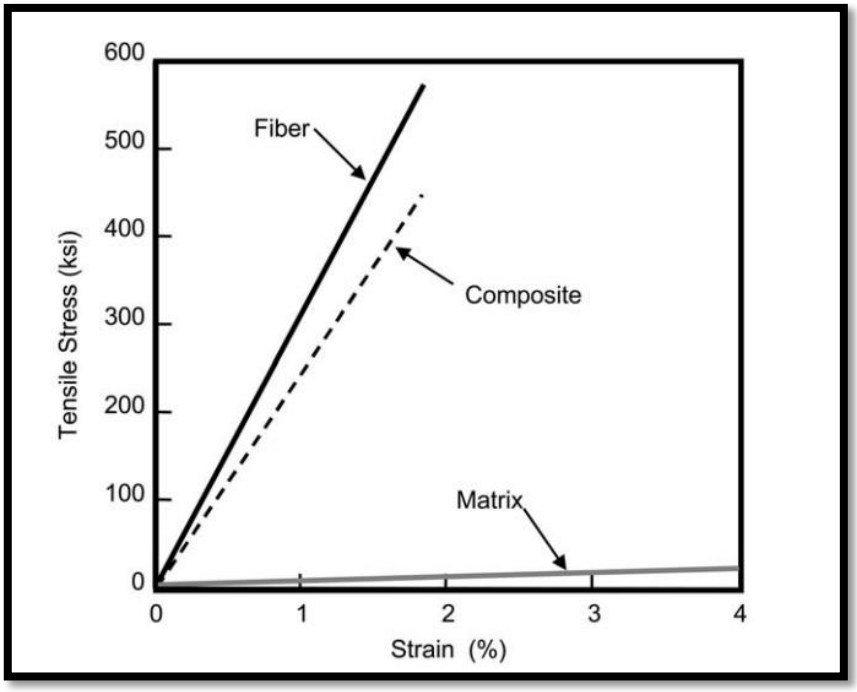

Figure 2.Comparison of tensile properties of fiber, matrix, and composite [1]

The tensile stress value are presented in kilopound per square inch (Ksi) where 1 ksi ~7 MPa. As it is shown in this figure 2 that the high-strength fiber can have a tensile strength of 500 ksi (3500 MPa) or more, a typical polymeric matrix normally has a tensile strength of only 5 to 10 ksi (35 to 70 MPa) and the composite has an intermediate tensile strength equal to 3100 MPa.

In composite materials there is the reinforcing phase which provides the strength and stiffness. In most cases, the reinforcement (carbon fibers, glass fibers, natural fibers…) is harder, stronger, and stiffer than the matrix which can be ceramics, metals or polymers.

Fibers are divided into continuous or discontinuous reinforcement. Continuous fibers have long aspect ratios* and they have a nonrandom orientation, while discontinuous fibers have short aspect ratios.

*Aspect ratio is defined as the ratio between the length and the diameter of the fiber (l/d).

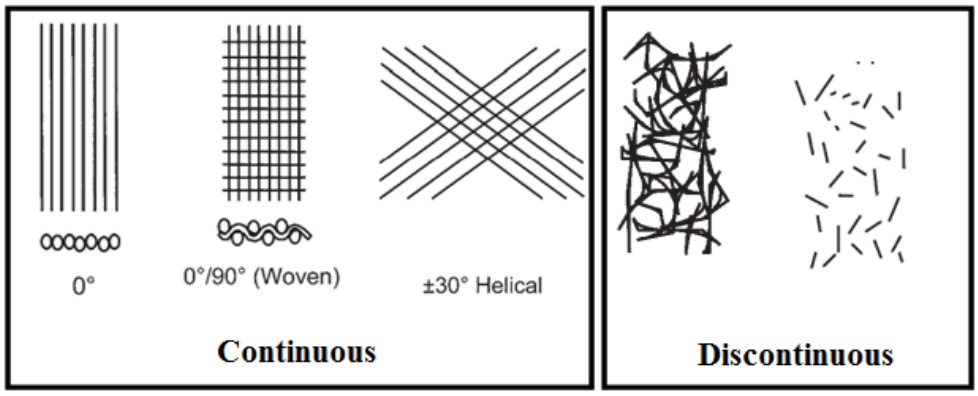

Figure 3.Typical reinforcement types [1]

2. Glass fibers (GF)

Fibers are the most common synthetic reinforcement due to their good properties which will dominate the characteristics and properties of the composites. Glass fibers are the most common of all reinforcing fibers for polymeric matrix. Their principal advantages are low cost, high tensile strength, good chemical resistance and excellent insulating properties.

Glass fiber bundles are consisting of a big number of extremely thin glass fibers, with a typically diameter between 3 to 20 µm [2], extracted from an inorganic product. In fact, according to the amount of the elements, like SiO_2, Al_2O_3,B_2O_3 …, different kind of glass fibers can be found such as those type represented in table 1;

Typical compositions of Glass Fibers (in wt%)						
Type	**S_iO_2**	**Al_2O_3**	**CaO**	**MgO**	**B_2O_3**	**Na_2O**
E-glass	54.5	14.5	17	4.5	8.5	0.5
S-glass	64	26	_	10	_	_

Table 1.Composition of S-glass and E-glass fibers [3]

The internal structure of glass fiber is a three dimensional as the long network of silicon, oxygen and other atoms are arranged randomly. Thus glass fibers are amorphous (non crystalline) and isotropic. S-glass is developed for aircraft components and E-glass which has very good insulation to electricity. [3]

In addition to these two types of glass fibers (E-glass and S-glass) there are other kind like A-glass which is used in the manufacture of process equipment, C-glass this kind of glass shows better resistance to chemical impact and AE-glass it is an alkali resistant glass. [4]

3. Epoxy resin (EP)

Epoxies are widely utilized for coatings, for structural applications and for microelectronic encapsulants. They are manufactured by reacting epichlorohydrin with bisphenol.

Those thermoset plastic which are cured under high temperature conditions, have high glass transition temperature. Their high modulus with low shrinkage makes them widely used as a matrix for composite applications. These materials have a large number of advantages including; relatively low cost, low density, good resistance to environment and they are a flame retardant ... [5,6]

The main functions of a matrix are the following: binds the reinforcements together, transfers stresses to the fibres, protects the reinforcements from environments and mechanical effects, provides the composite with a solid form, controls the transverse properties,, holds reinforcing fibres in the desired orientation. [7]

4. Glass fiber epoxy laminate (GF/EP)

Both glass fibers and polymer epoxy resin matrix are chemically bonded in order to form the composite material. These two materials act together, each overcoming the deficits of the other. Whereas the plastic resins are strong in compressive loading and relatively weak in tensile strength, the glass fibers are very strong in traction but tend not to resist compression. By combining the two materials, the composite becomes a material that resists both compressive and tensile forces as well.

The most common form in fiber-reinforced composite are used in structural application is called laminate. This laminate is made by stacking a number of thin layers of fiber and matrix (epoxy) and consolidating them into the desired thickness. The mechanical performance of the laminate depends of the amount of the fibers and their special orientation.

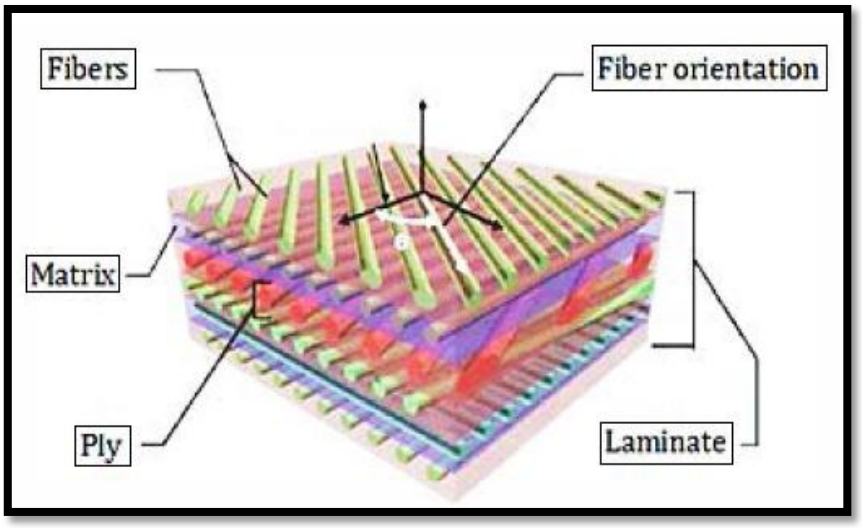

Figure 5.Laminated composite [8]

5. Adhesion between glass fibers and epoxy resin Glass

In order to prevent fracture and ensure sufficient lubrication, all glass fibers used in ply production have a form of sizing. This sizing is subsequently removed by a thermal decomposition process and the fabric is coated with a silane* coupling agent to provide a chemical coupling between the glass surface and the resin matrix.

*The silane coupling agent has the ability to form a durable bond between organic and inorganic materials in order to incorporate the bulk properties of different phases into a uniform composite structure.

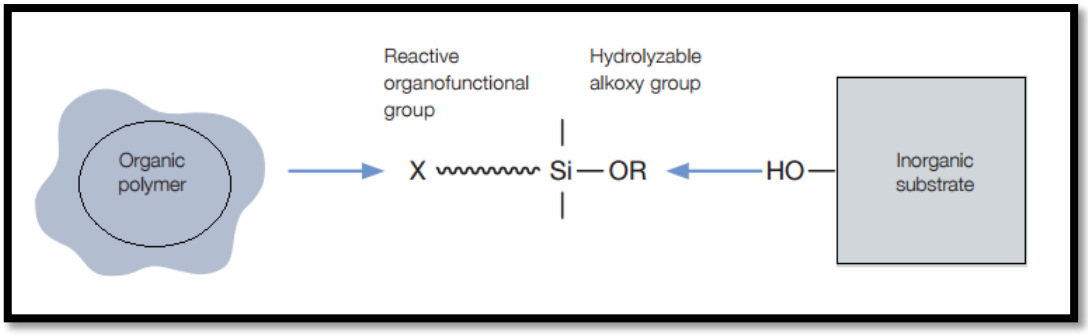

Figure 6.The functional groups of the silane coupling agent [9]

These coupling agents will influence fiber-resin interaction through changes in surface properties such as surface energy and bonding site availability. [10]

6. Damage in laminate composite

6.1. Damage modes

Although epoxy plus glass fiber composite materials have high stiffness and high strength, they are brittle and they have poor resistance to crack initiation and growth [11] those damages are essentially caused by the complex loading supported by the laminates during the service:

- For unidirectional composite the damage can be shown, as following, according to the load direction: [12]

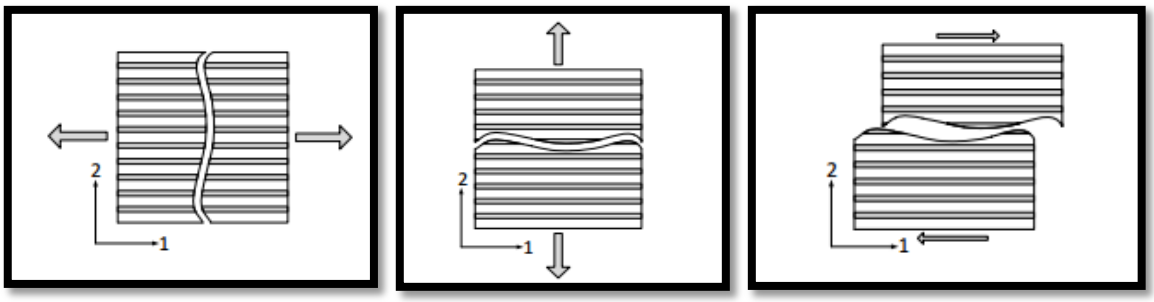

Figure 7.(a) Mode I fracture perpendicular to the fiber direction.(b) Mode I fracture parallel to the fiber direction. (c) Mode II fracture parallel to the fiber direction

- For the multidirectional composite the damage can be represented as following:

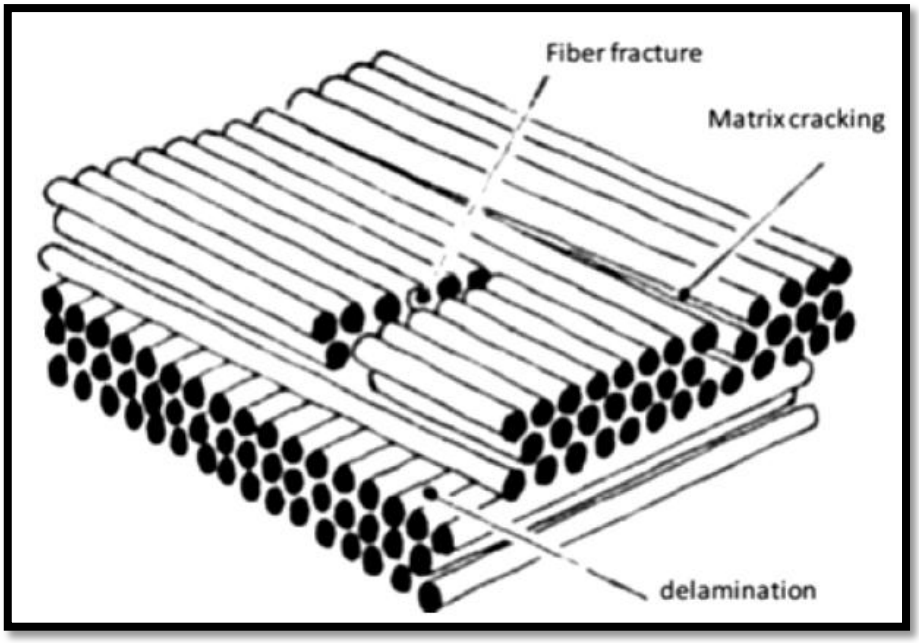

Figure 8.Damage mechanisms of laminated composite structure subjected to impact loading [8]

- Matrix cracks: They take place due to the big difference on properties between matrix and fibers and it happens generally parallel with fiber direction of plies. Several studies have shown that the damage in composite materials is always initiated by matrix cracks and subsequently develops as the failure of delamination.
- Delamination: It is a mode of failure of laminated composite materials, which leads to the separation of the layers of reinforcement or plies. It could reduce the role of fiber strength and make the weaker matrix properties handle the structural strength.
- Fiber fracture : This damage mode can take place during longitudinal tension or compression and the energy consumed by these failure processes is much larger than the matrix or matrix-fibre bond failure.[8,13]

6.2. Initiation and propagation of damage

Some studies were ignoring the fiber/matrix microstructure and considering the layer in the laminate a homogenous material, the initiation of the damage is represented as meso-scale damage entities which reach a certain size and start to grow in the layer thickness direction.

This meso-scale damage continue to grow in the thickness direction and it will be arrested when they approaches the interface of the neighbor layer.

From stress point of view, the damage initiate in the edge of the specimen where the stress concentration is higher than inside of it; those area characterized by the limited space between fibers which lead to the decrease of the interface and resin failure properties.[14]

The laminate failure doesn't take place when just one ply has failed because the rest of layers may hold the whole load.

6.3.Manufacturing defects

The damage in the composite doesn't come only from loading but also it comes from the manufacturing process. Manufacturing-induced defects widely exist in fiber-reinforced polymeric composites, the most common defect are listed in table 2;

Location	Manufacturing defects
Matrix	Void, porosity, resin rich area, incompletely cured matrix
Fiber	Fiber misalignment, dry zone, fiber defects
Fiber/Matrix interface	Deboning
Interface between plies	Delamination

Table 2. The common manufacturing defects in fiber-reinforced composite laminates

Voids are of the most common defects in any manufacturing process; they can form during curing process from to origins: [15]

- The gas entrapped during lay-up for prepreg based processes.
- The volatiles and gas from the moisture forming at relatively high curing temperature

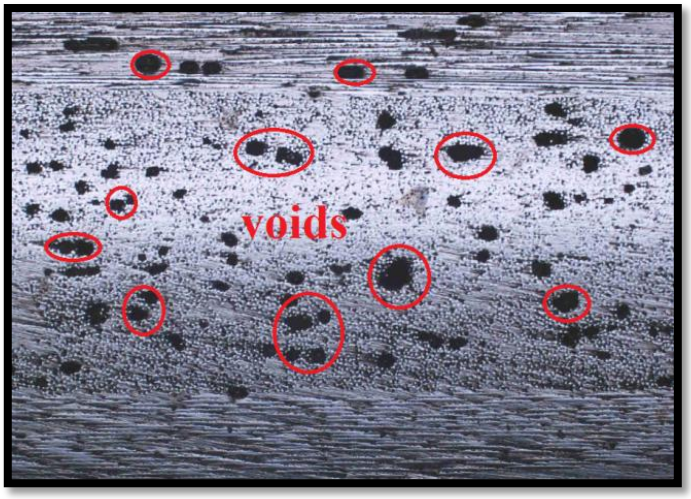

Figure 10.Microscope observation of voids comes from manufacturing

7. Static tensile test

7.1.Influence of the fiber orientation on the mechanical properties of the laminate

Three polypropylene/glass-fiber thermoplastic composites specimens, who differ by the arrangement of the layers, were subjected to static tensile test using Instron Universal Testing machine in order to compare some mechanical properties. The results are obtained with a grip displacement rate of 2000 mm/min. From the experimental data represented by the next tabled values it is shown that the 0° laminate exhibits the higher stiffness and strength comparing to

+45°/0°/-45° and +30°/-30°/0° laminates. This is due to the difference in the failure mechanisms in each case [16]:

- For the 0° laminate the failure was dominated by the fracture of axially aligned fibers
- For +45°/0°/-45° and +30°/-30°/0° laminates the failure was dominated by the delamination of inclinated fiber layers.

Laminates	Ultimate strength (MPa)	Stiffness (MPa)
0	438	0.015916
+30°/-30°/0°	211	0.009113
+45°/0°/-45°	196	0.010138

Table 3.Experimental mechanical properties

The two different fracture modes exhibited during static testing are shown in figure 11[16];

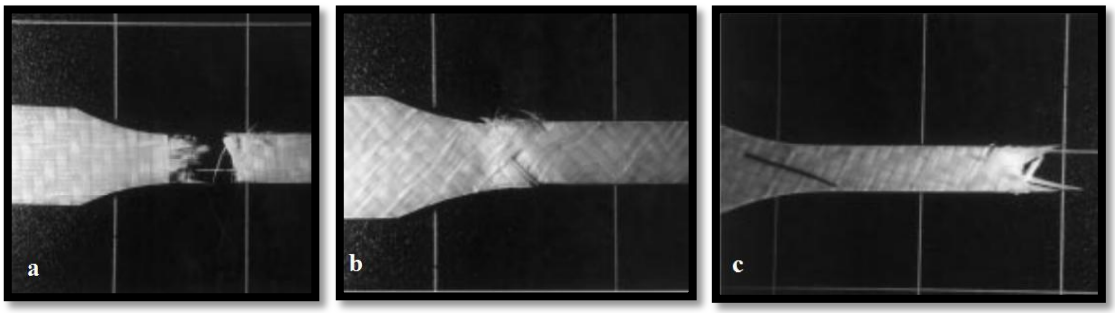

Figure 11.Fracture get after performing static test for three different fiber's orientation. (a) 0°, (b) +45°/0°/-45°, (c) +30°/-30°/0°

7.2.Temperature effect on the mechanical properties of the laminate

Some static tensile tests were done by Mohammad A Torabizadeh for the unidirectional laminate using low temperature, in order to determine the effect of this parameter on the tensile strength, Young modulus and ultimate strain of those unidirectional composites. The test was done at three different temperatures; 20°C (room temperature), -20°C and -60°C and the curves of the longitudinal tensile stress versus strain were plotted in figure 12 [17];

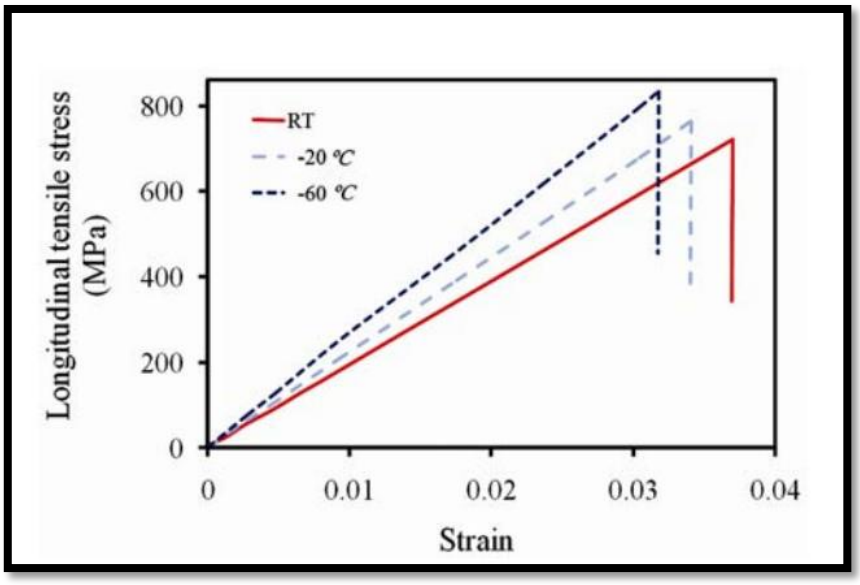

Figure 12.Typical stress-strain behavior of unidirectional laminate under tensile loads in longitudinal direction at 20°C, -20°C and -60°C. [17]

From the previous curve, the laminates exhibit, at three different temperatures, a linear elastic behavior until failure; while the decrease of the temperature is followed by the increase of the slope. It was noted that the reduction of the failure strain was a slight reduction (from 0.037 at room temperature to 0.032 at -60°C). However, the Young modulus and the tensile strength increase when the temperature decreases. So the stiffness of the fiber rapidly increased within a temperature range from room temperature to -60°C. [17]

8. Fatigue tensile test

8.1.The influence of matrix nature in the fatigue failure of the composite

One way to improve the mechanical properties of the composites is to improve properties of epoxy matrix by incorporating various types of micro and nano-sized particulate and fibrous in the resin and it will be a hybrid matrix.

Two kinds of glass fiber composite, one is reinforced neat epoxy and the other is reinforced hybrid epoxy, were subjected to a tensile fatigue test at stress ratio R=0.1 and σ_{max}= 150 MPa.

After performing the fatigue test, the curves of the normalized stiffness as a function of number of cycles were represented in figure 13[18] for the two composites as following;

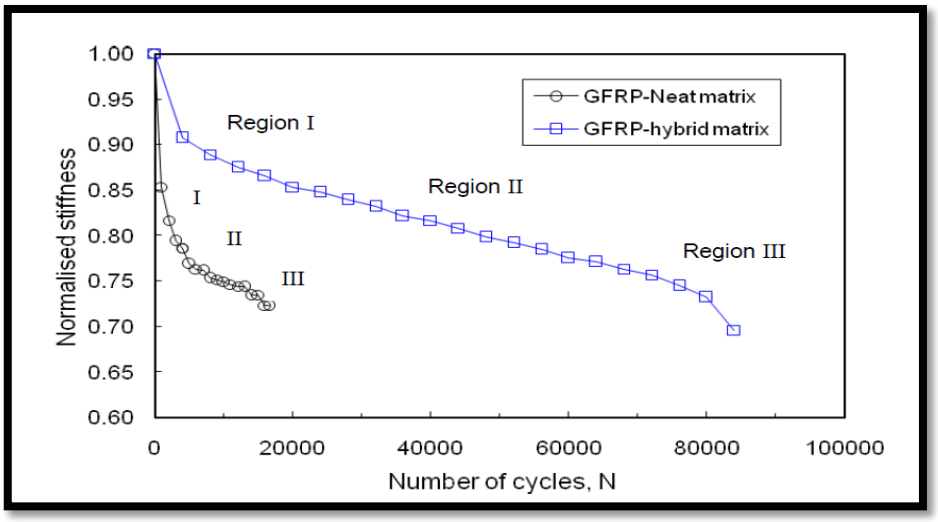

Figure 13.The normalized stiffness variation with fatigue cycling in GFRP composite with neat and hybrid epoxy matrix [18]

Both, the GFR hybrid matrix and the GFR neat matrix exhibit the same way of evolution; the stiffness decreases when the number of cycles increases. It may be noted that the stiffness reduction in region I and region II was quite steep and significant in neat matrix GFRP composite when compared to GFRP with hybrid epoxy matrix.

This reduction can be explained throw the accumulation of damage which comes from the high stress during the fatigue test, this damage evolution can be represented by the crack density (number of cracks per unit of length) versus number of cycles curves in figure 14;

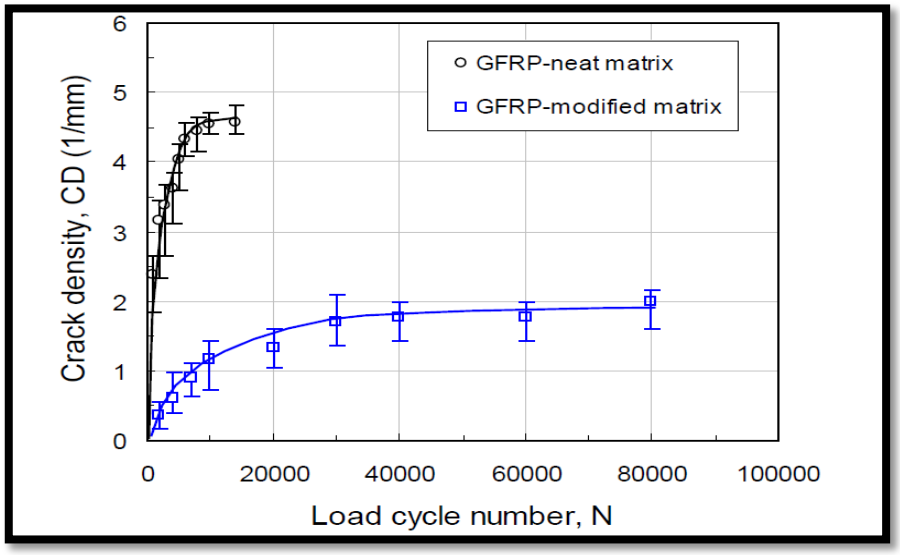

Figure 14.The variation of crack density with fatigue cycles in GFRP composite with neat and hybrid matrix [18]

The crack densities increase with the increasing number of cycles which lead to a continuous decrease in the global stiffness of the composite as it was shown in the previous graph.

The crack density of the glass fiber reinforced neat matrix is greater than the crack density of the glass fiber reinforced hybrid matrix and it reached its maximum even at less than 20000 cycles while that of the reinforced hybrid matrix reached its maximum after 80000 cycles. So the modified matrix has mechanical properties better than the neat one, it enhance the fatigue life of the composite. [18]

Chapter 3:

Materials: Specimen's preparation

In this project the cross-ply $[0_2,90_2]_s$ were made in the laboratory of the university starting from the composite laminate manufacturing until the tabs gluing. In order to get specimen, ready to undergo the mechanical tests, several intermediate steps, described in the following part, were done.

1. The laminate preparation

From the glass fiber/epoxy pre-impregnated* sheets of fiber, small squares with 20 cm length were cut. Then those squares will be placed one over the other in order the make the lay-up wanted (in our case $[0_2,90_2]_s$ is the lay-up used).

*Material in sheet form impregnated with resin. It may be stored in the refrigerator before use.

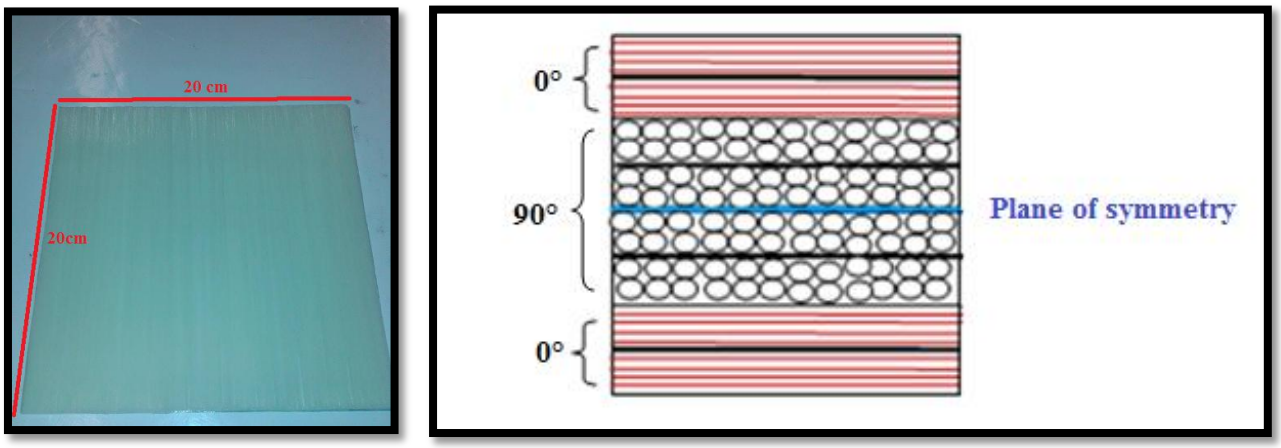

Figure 15.(a) GF/ EP uncured laminate. (b) Laminate's layers disposition in cross-ply $[0_2,90_2]_s$

The laminate composite wanted was a cross ply laminate consisting of 8 layers of glass fiber/epoxy with alternating orientations of 0° and 90°. A release film was used to cover both sides of the laminate. This film contains holes but their diameter and spacing can vary depending on the amount of resin flow desired.

The covered laminate was placed into metallic plate painted with release agent (avoids that the laminate stick), a breath film was used also to maintain a breath path throughout the bag to

the vacuum source so volatiles and air can escape and pressure can be applied to the laminate as it is showing in the next figure;

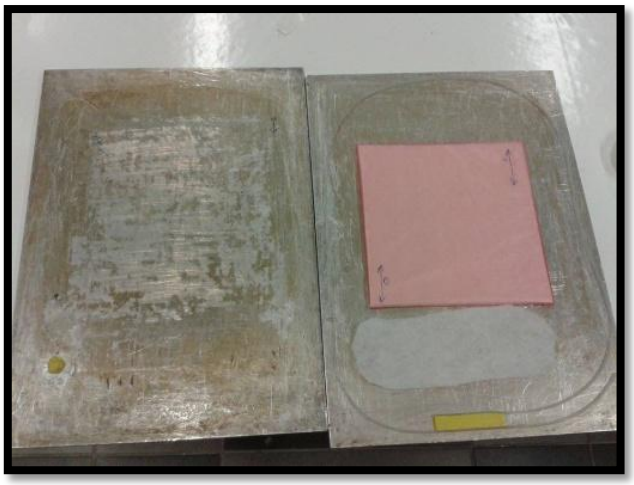

Figure 16.Covered laminate placed into metallic plate

In the following step, the vacuum pump connected to the plate, was taken to the hot pressure machine to start the curing process during one hour in 125°C.

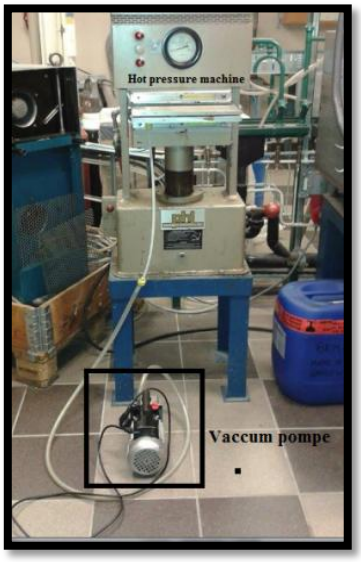

Figure 17.The curing process

The cured laminate was cut in small specimens with a width between 10 mm 13mm.Then; the specimens were polished in order to do some optical microscopy observations. Finally, the tabs are glued to obtain specimens ready to undergo the mechanical tests.

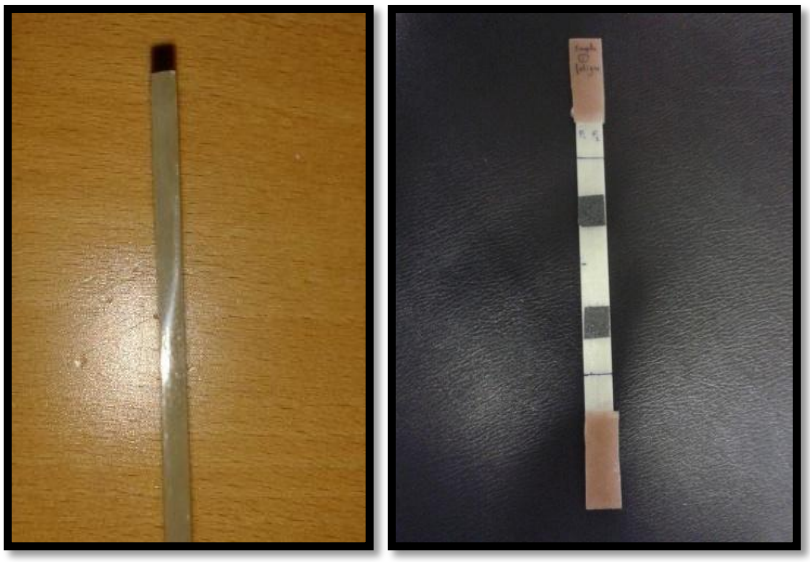

Figure 18. (a) Bright edge gets after polishing step.(b)Specimen ready for testing

2. Optical microscope observation

The optical microscope observation of un-tested specimens was done. The arrangement of the different lay-up of the composite laminate was represented as follows;

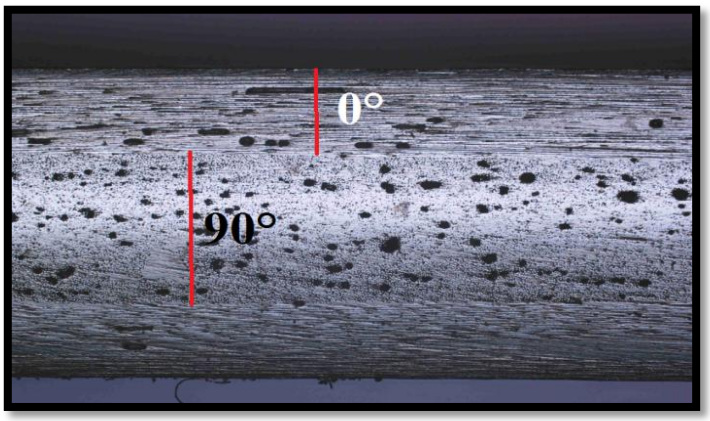

Figure 19.Microscope observation of untested $[0_2,90_2]_s$ edge

From this microscope observation it was seen that the 90°-layer contained more voids than the 0°-layer. The voids formed during the manufacturing process. Those excluded area were fibreless, so they can influence the mechanical properties of the laminate.

The content of voids was determined using the microscope for untested specimen;

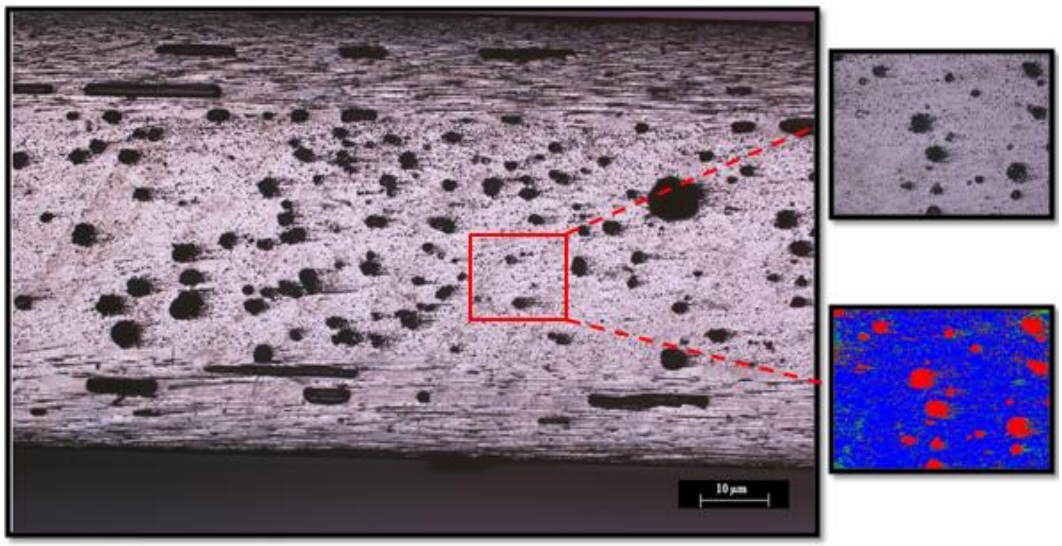

Figure 20.Estimation of the voids area fraction in small edge's area

The estimation was that into a surface area equal to 4.06 mm^2 the voids percentage is 13.5 % of the total area.

Chapter 4:

Quasi static tensile test

1. Methodology

The static test was done with the QUASI-STATIC tensile machine INSTRON 3333.This testing machine has 10 KN as maximum load;

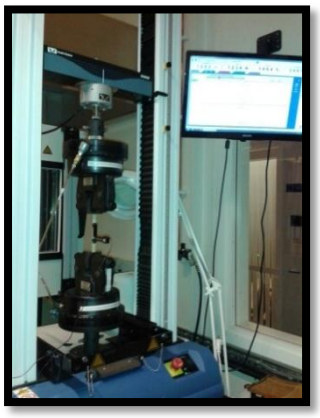

Figure 21.Quasi-static tensile machine INSTRON 3333

This static tensile test follows the strain ramp represented in the next graph;

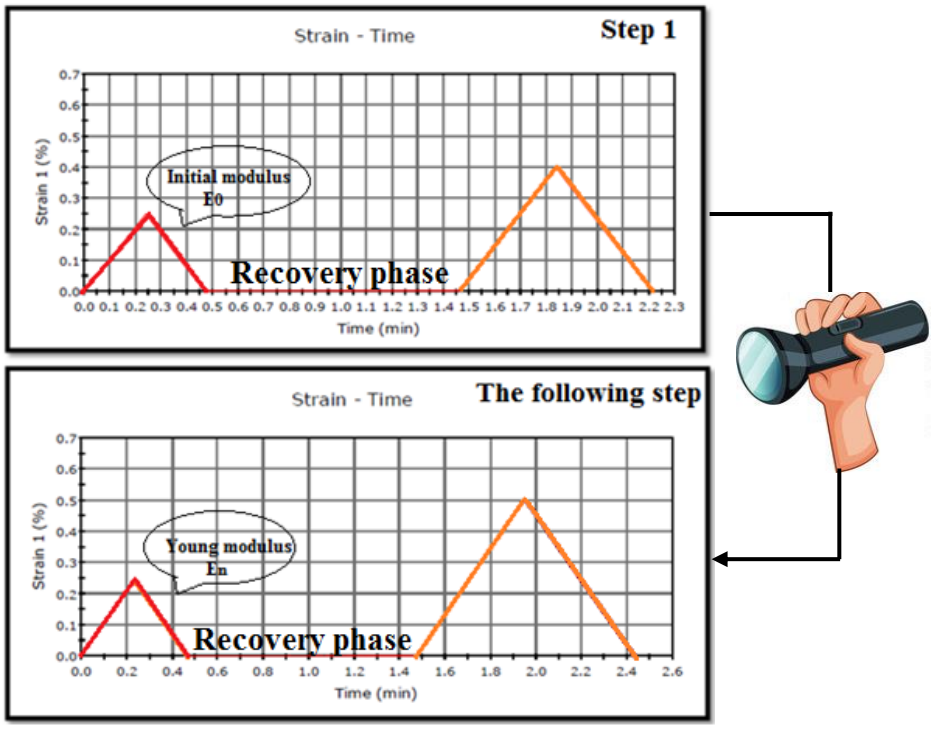

Figure 22.Strain versus time curves for the first and the second step of the static test.

The specimens were loaded until 0.25 % of strain, then unloaded. The loading and unloading part were represented in red (figure 22), they are used to do the stiffness measurement. The Young's modulus was the slope of the stress versus strain curves plotted using the experimental data. The initial Young modulus was measured at the first step where there were no cracks and no damage.

After a recovery phase, of 1 minute and at the strain almost 0%, the specimens were loaded again until a high strain level which increases from step to another; at each step the strain increases by 0.1 % until the failure of the specimen or until reaching the maximum load that can apply the testing machine.

After each step, the specimen was not dismounted and the matrix cracks in the marked area (100 mm as length) in the two edges were counted by simple optical observation using the reflected light because of the translucent nature of the glass fiber/epoxy composite.

2. Weibull's statistic

After performing the uni-axial loading, the experimental data were analyzed in order to get the Weibull's parameters. As the transverse tensile stresses for responsible cracking in the 90° layers we assumed a statistical distribution of the probability of failure at certain stress level presented by the equation (1).

For this assumption the next properties were used for all specimens' calculation:

$$\begin{cases} E_L = 37.4 \text{ GPa} \\ E_T = 9.34 \text{ GPa} \\ G_{LT} = 3.5 \text{ GPa} \\ \alpha_L = 7.03 \text{ e-6 (1/C)} \\ \alpha_T = 40.187 \text{ e-6 (1/C)} \\ \nu = 0.3 \end{cases}$$

Indeed the E_L, E_T and G_{LT} are obtained experimentally from the slope of the stress versus strain curves in static tensile test for lay-up $[0]_4$, lay-up $[90]_6$ and lay-up $[\pm 45]$s respectively.

The Poison's ratio is also obtained experimentally as the slope of the transverse strain versus longitudinal strain curve.

The damaged layer, 90°, will be divided into small square shape elements where each element contains only one crack and the distance between two cracks can't be lower than the thickness of the damaged layer:

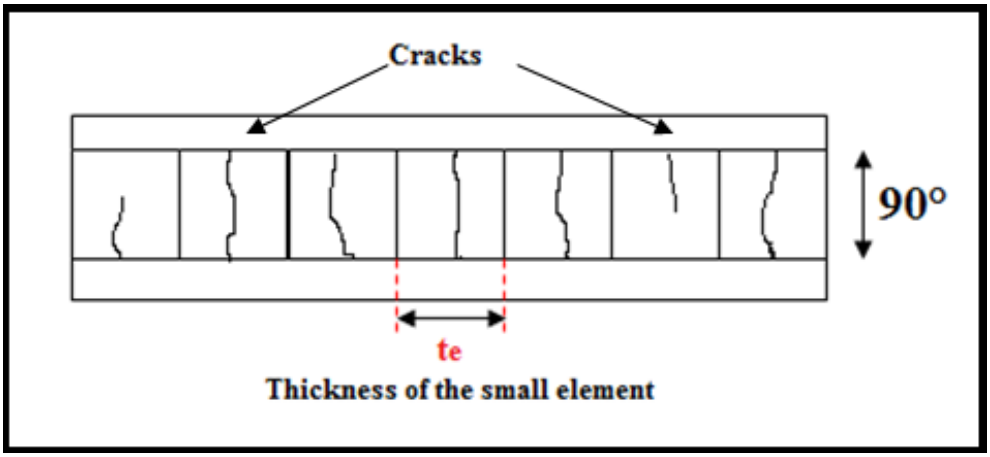

Figure 23.Schematization of layer 90° divided in small failed elements

The individual intra-laminar cracking initiation stress can be described from the Weibull strength distribution in such a way;

$$P_f = 1 - \exp\left[\frac{V}{V_0}\left(\frac{\sigma_T}{\sigma_0}\right)^n\right] \qquad (1)$$

Where P_f is the probability of failure of the small element, σ_T is the thermo-mechanical transverse stress and σ_0, n are respectively the scale and the shape Weibull's parameters. V_0 is the element volume and V is the volume of considered element.

$$\text{Ln}\left(-\ln\left(1-P_f\right)\right) = \ln\left(\frac{V}{V_0}\right) + n\,\text{Ln}\left(\frac{\sigma_T^{90}}{\sigma_0}\right) \qquad (2)$$

The estimation is that V_0=V, so the shape Weibull's parameter is the slope of the ln (-ln(1-P_f) versus ln(stress) curve. Where ln is the logarithm function.

This probability of failure at certain stress P_f (σ_T) can be defined also as the ratio between the experimental crack density (ρ) and the maximum crack density (ρ_{max})

$$P_f = \frac{\rho}{\rho_{max}} \qquad (3)$$

Where $\rho_{max} = \frac{maximum\ \ number\ \ of\ \ craks}{lengt\,h}$

During the manufacturing process there is the curing step, during this step, thermal stresses develop. After performing a tensile test the total transverse stress is defined as following:

$$\sigma_T = \sigma_T^{90\ mech} + \sigma_T^{90\ thermal} \quad (4)$$

$\sigma_T^{90\ mech}$ comes from the mechanical loading during the test and $\sigma_T^{90\ thermal}$ is due to difference of the thermal extension between layers also during the curing. Those stresses were calculated using the LAP program. This LAP performs a succession of operations according to the classical laminate theory

- The stiffness matrix Q of the composite material is introduced in the following

$$\begin{Bmatrix} \sigma_1 \\ \sigma_2 \\ \sigma_6 \end{Bmatrix} = \begin{pmatrix} Q_{11} & Q_{12} & 0 \\ Q_{21} & Q_{22} & 0 \\ 0 & 0 & Q_{66} \end{pmatrix} \begin{Bmatrix} \varepsilon_1 \\ \varepsilon_2 \\ \varepsilon_6 \end{Bmatrix} \quad (5)$$

Where

$$Q_{11} = \frac{S_{22}}{S_{11}S_{22} - S_{12}^2} \qquad Q_{12} = Q_{21} = -\frac{S_{12}}{S_{11}S_{22} - S_{12}^2}$$

$$Q_{22} = \frac{S_{11}}{S_{11}S_{22} - S_{12}^2} \qquad Q_{66} = \frac{1}{S_{66}}$$

Using matrix notation, equation (3) can be written

$$\{\sigma\} = [Q]\{\varepsilon\} \quad (6)$$

- Calculation of the transformation matrix [T] in order to move from local to global system

$$[T] = \begin{pmatrix} m^2 & n^2 & +2mn \\ n^2 & m^2 & -2mn \\ -mn & +mn & m^2\text{-}n^2 \end{pmatrix} \quad (7)$$

Where m= cos θ and n=sin θ

- Calculation of $\overline{Q}$ matrix, stiffness matrix in global system

$$[\overline{Q}] = [T]^{-1}\,[Q]\,([T]^{-1})^T \quad (8)$$

$$[T]^{-1} = \begin{pmatrix} m^2 & n^2 & -2mn \\ n^2 & m^2 & +2mn \\ +mn & -mn & m^2\text{-}n^2 \end{pmatrix} \quad (9)$$

$[T]^{-1}$: Transformation from the global system to the local one.

Classical Laminate Theory: This **CLT** is the basic theory for composite which is used to calculate the properties of the laminate when the properties of each constituent (matrix, fibers) are known. It is based on the following assumptions:

- ✓ The thickness of each ply is very small as compared with other dimensions.
- ✓ Each ply is a plate with uniform thickness
- ✓ The bond between two plies is perfect; plies cannot slip. The laminate acts as an anisotropic unit.

The first calculation get through this theory is:

- ❖ The extensional stiffness matrix of the laminate

$$[A]= \sum_{i=1}^{n}[\overline{Q}]_i t_i \qquad (10)$$

- ❖ The coupling stiffness matrix of the laminate

$$[B]= \sum_{i=1}^{n}[Q]_i \frac{\overline{zi^2 - z_{i-1}^2}}{2} \qquad (11)$$

- ❖ The bending stiffness matrix defined by:

$$[D]= \sum_{i=1}^{n}[\overline{Q}]_i \frac{zi^3 - z_{i-1}^3}{3} \qquad (12)$$

The compact form of the constitutive relationship for laminate is represented as following

$$\begin{Bmatrix} N \\ M \end{Bmatrix} = \begin{bmatrix} A & B \\ B & D \end{bmatrix} \begin{Bmatrix} \varepsilon_0 \\ K \end{Bmatrix} \qquad (13)$$

Where $N= \frac{F_x}{Width}$ Force per unit of width of the specimen.

This equation is an expression of six linear relationships between six force and moment components from one side and six midplane strain and curvature components from another side.

The laminate used in this project is symmetric laminate that's why the coupling stiffness matrix and K equal to 0. ([B]≡ 0, K=0)

When we applied N, the LAP gives us the strain value in the global system and in order to get the strain value on the local system, the transformation matrix was used (equation (5)). Then the local stresses were given as following;

$$\sigma_L = Q_{11}\varepsilon_L + Q_{12}\varepsilon_T$$

$$\sigma_T = Q_{12}\varepsilon_L + Q_{22}\varepsilon_T \qquad (14)$$

$$\sigma_{LT} = Q_{66}\,\gamma_{LT}$$

After calculation, the scale and shape Weibull's parameters were obtained, the average strength can be find as following;

$$\overline{\sigma} = \sigma_0 \Gamma\left(1+\frac{1}{n}\right) \qquad (15)$$

3. Results and discussion

3.1. Stiffness reduction

Three specimens made from the same lay-up, were subjected to the static tensile test, they had approximately the same thickness and width:

Specimens	Initial elastic modulus (GPa)	Thickness (mm)	Width (mm)
1	21	2.71	11.52
2	22.68	2.68	10.35
3	21.46	2.65	10.82

Table 4.Initial elastic modulus, thickness and width of 3 specimens

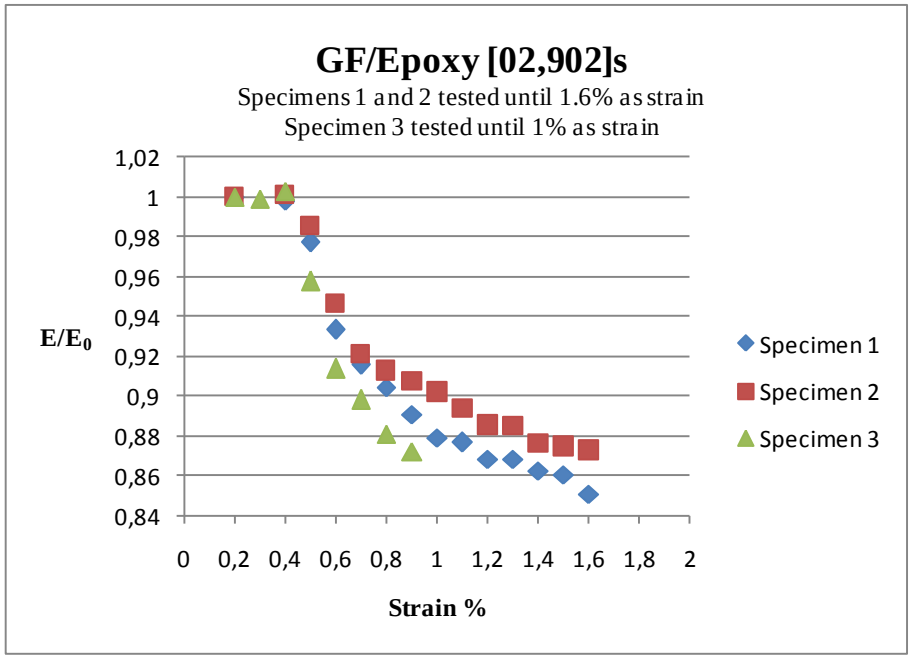

Figure 23.Stiffness reduction for three specimens subjected to static tensile test

Specimens 1 and 2 were tested until 1.7% and they didn't break. They need more than 332 MPa of tensile stress to be broken. Specimen 3 was tested until 1 % as strain and it didn't fail also.

For this these specimens, after reaching 0.4 % of strain the initiation and the accumulation of cracks took place. The stiffness of the 90°-layer and as well the stiffness of the whole laminate was decreasing.

The number of visible damage in 90 °-layers were represented with crack density (CD) value, which was defined as the number of cracks per unit length. It may be noted that there was an uncertainty on the accuracy of such measurements (count the CD) since the cracks were counted visually. Despite the specimen needed a load greater than 9000 N to be broken, their Young modulus was influenced by the crack density and it increased gradually after each test step:

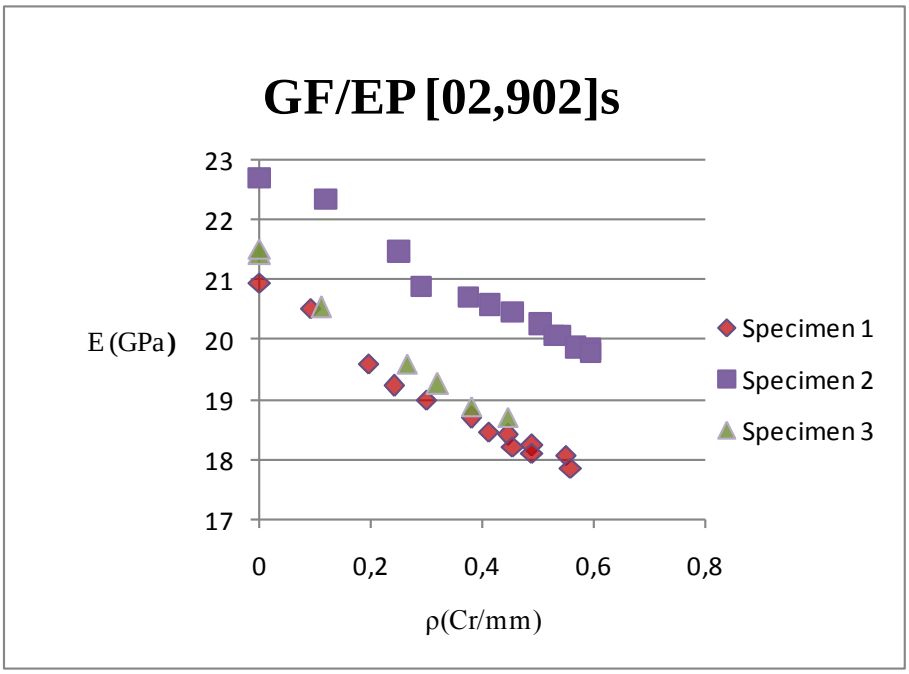

Figure 24.Stiffness reduction versus crack density

From the two previous curves, it was noted that the specimen stiffness's decrease with the increasing value of both the crack density and the strain. This stiffness reduction was about 16 %, 13% and 13 % respectively for specimen 1, 2 and 3.Moreover, even the specimens were obtained from the same plate but they hadn't the same mechanical properties and this could be due to the difference percentage of voids coming from manufacturing process and the difference of volume fraction.

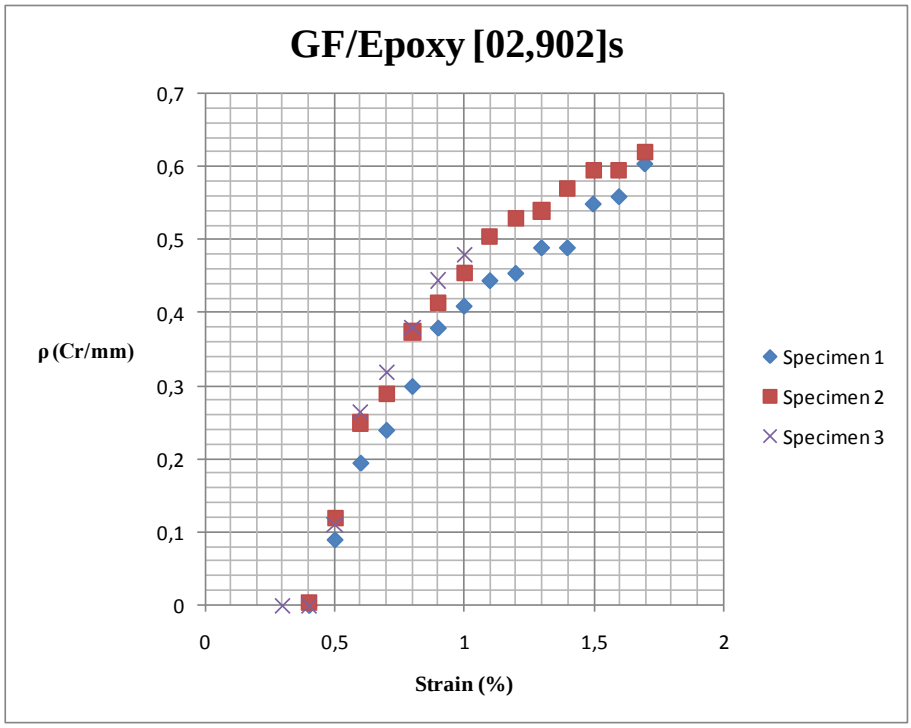

Figure 25.Crack density as a function of strain

The crack density increases with the increasing strain level. For strain greater than 1 % it can be shown from this graph that there was cracks concentration for both specimens 1 and 2.Sometimes at a higher strain value, the number of cracks was quit the same, but there was a stiffness reduction, this reduction could be due to the apparition of another damage mode: the delamination.

3.2. Optical microscope observation after performing static tensile test

Usually in the tensile tests the cracks cover the whole thickness of the layer and propagate over the whole width of the specimen. Since the number of cracks increases it can initiate other damage modes, such as local delamination at the intralaminar crack tip, and fiber breaks.[21]

Generally the study of the transverse cracking in multidirectional laminates was performed on cross-ply laminates [0°, 90°], where 0° was the outer layer and 90° was the inside layer. When this laminates were subjected to uni-axial tensile loading the 90°-layer, where the fibers were oriented perpendicularly to the load direction, was the first affected by cracks because the properties of fibers in longitudinal direction were superior compared to the transverse ones. Moreover, when the strain was increased the crack spacing decreases and when the materials were subjected to a high stress the delamination or damage in the longitudinal 0 ° plies could be generated.

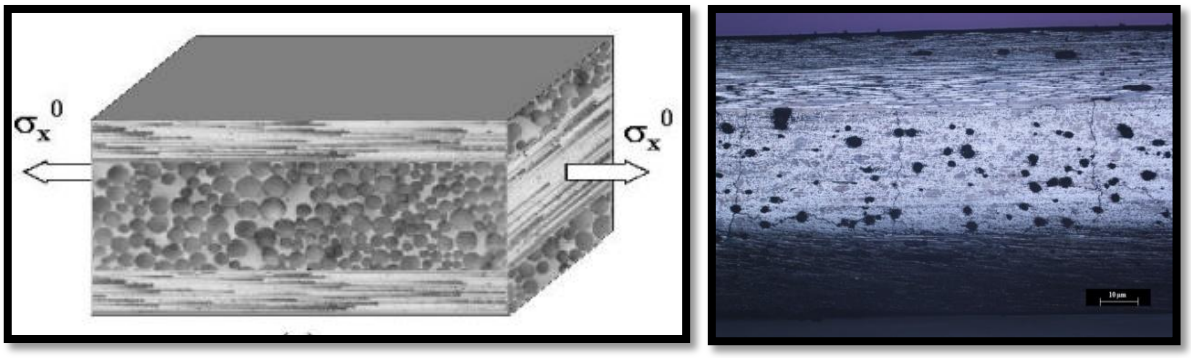

Figure 26.(a) Cross-ply laminate subjected to uni-axial loading [19]. (b) Resulting damage

Using a higher magnification with the microscope, the damage can be shown as following;

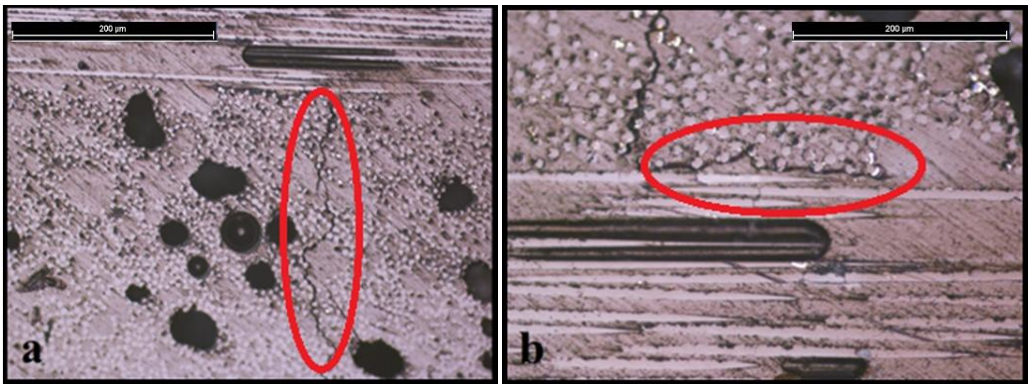

Figure 27.(a) Matrix crack. (b) Delamination

Those pictures were taken for a specimen 2 subjected to static tensile test until 1.7%. The two edges contain 62 cracks distributed in the marked area (length=100mm) throughout the 90°-layer. As first step the edges showed the appearances of matrix cracks (figure a) which crossing transversally the 90°-layer and initiate delamination on their tips between the layers 90° and 0° (figure b).

3.3. Weibull's distribution

After performing the static tensile test the experimental data were analyzed in order to get the Weibull's shape and scale parameters. The 3 specimens will have the same properties already mentioned in the methodology section.

As the specimen 1 and 2 are subjected to the same strain level (1.7%) their probability of failure versus transverse stress can be represented in the same curve:

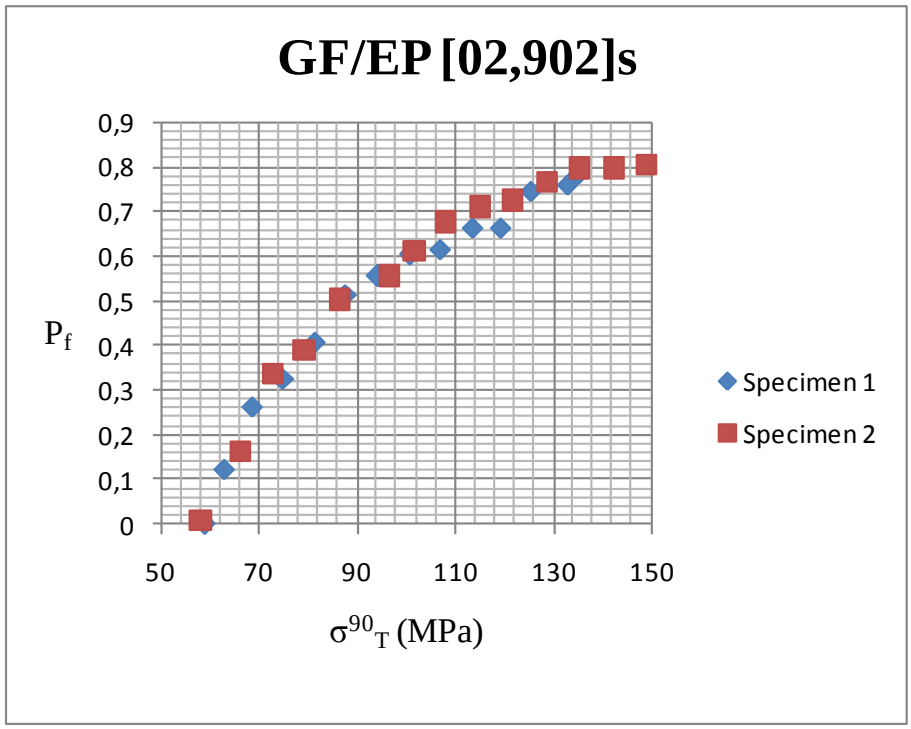

Figure 28.Probability of failure as a function of transverse stress for specimens 1 and 2

The probability of intralaminar cracking in 90-layer increases with the increasing thermo-mechanical transverse stress value.

The Weibull's parameters (n and σ_0) and the average strength of each specimen were determined through the following curves separately;

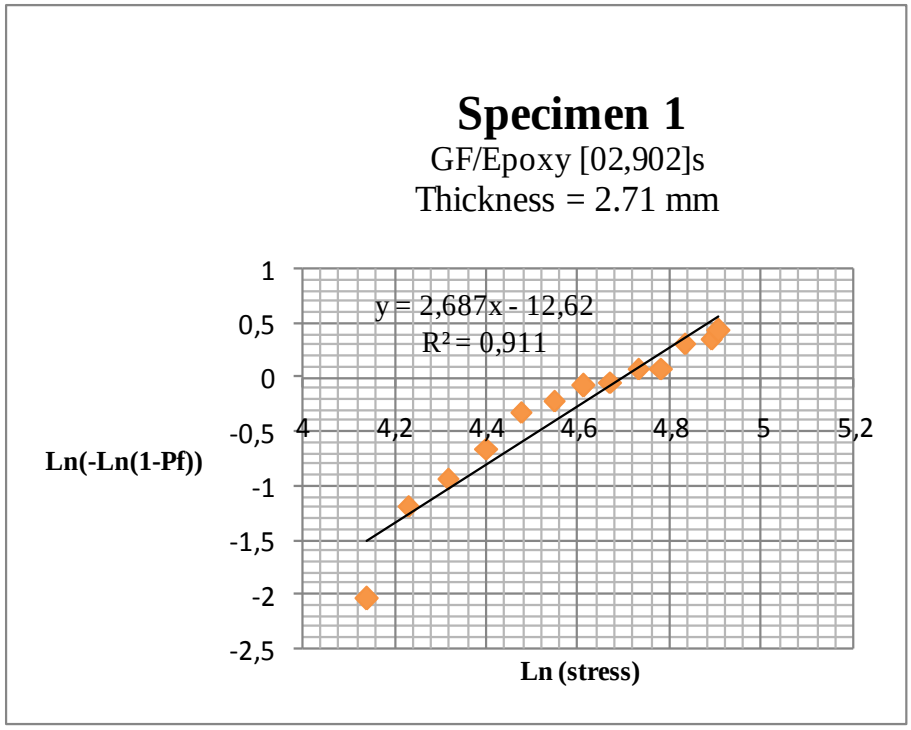

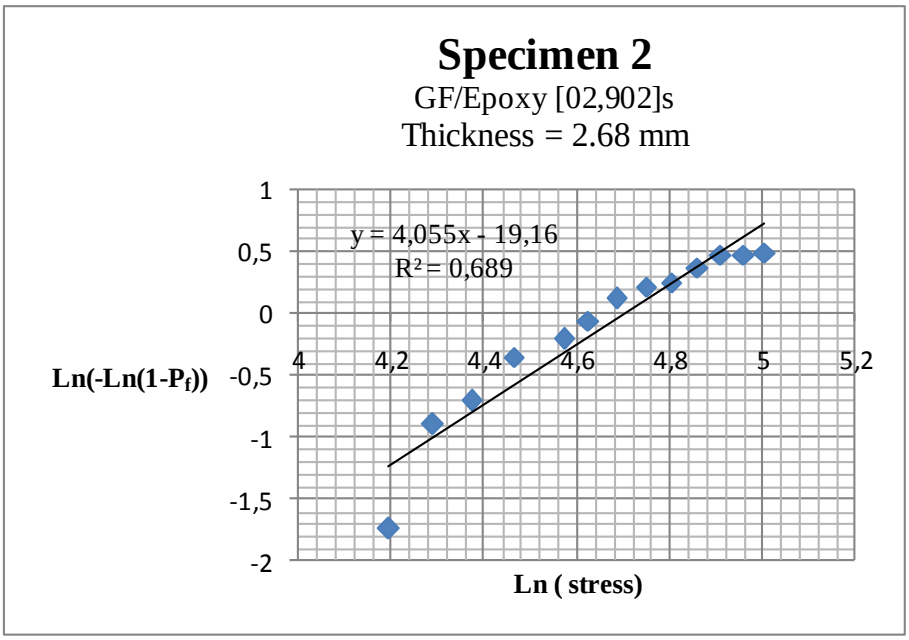

Figure 29. Ln(-ln(1-P_f)) versus Ln (stress)

n_1 = 2.687	σ_{01} = 109.583 MPa	$\overline{\sigma_{01}}$ = 97.43 MPa
n_2 = 4.055	σ_{02} = 112.734 MPa	$\overline{\sigma_{02}}$ = 102.261 MPa

The specimen 3 was tested until 1% strain. Its Weibull's parameters and average stress were obtained as following;

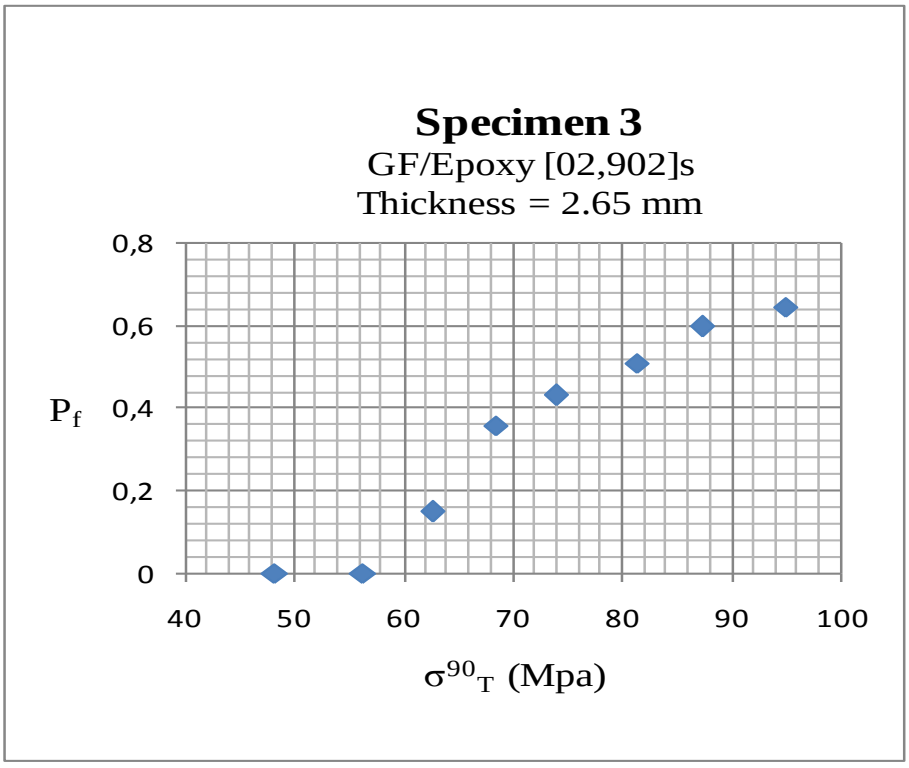

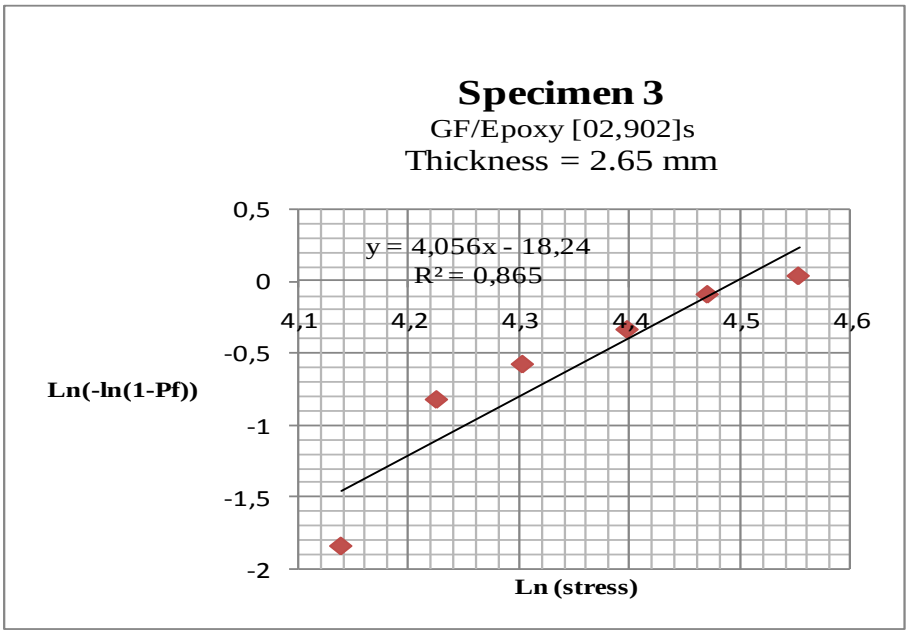

Figure 30.(a) Probability of intra-laminar cracking in 90° layer as a function of thermo-mechanical transverse stress. (b) Ln(-ln(1-P_f)) versus Ln (stress)

n_3 = 4.056	σ_{03} = 89.751 MPa	$\overline{\sigma_{03}}$ = 81.415 MPa

As this specimen tested only until 1% as strain, it has lower σ_{03} comparing to the other two specimens. Although the reached strain was not too large, the specimen showed a stiffness reduction by 13%;

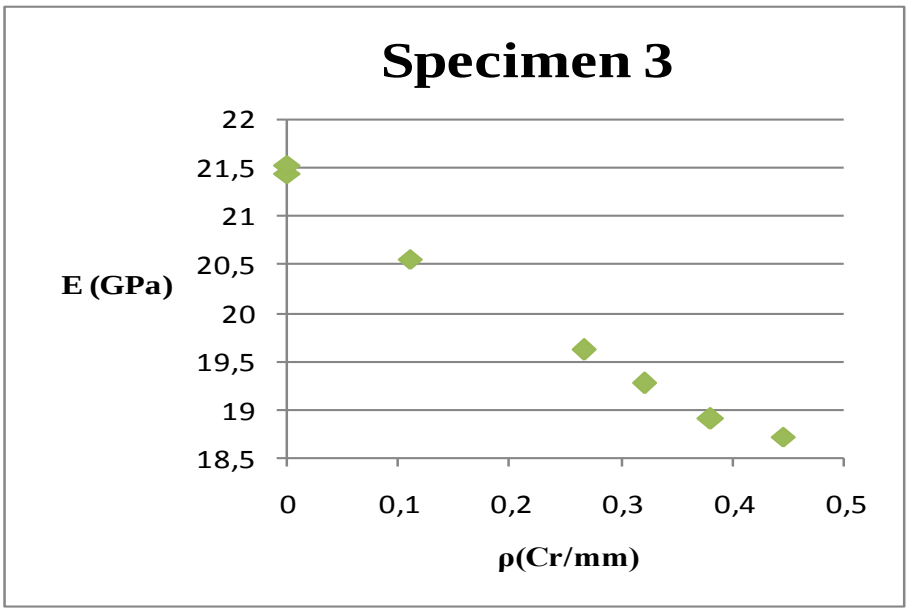

Figure 31.Young modulus as function of crack density

Chapter 5:

Fatigue tensile test

1. Methodology

The fatigue tensile test was a uni-axial tensile loading (load controlled test), where the maximum stress corresponding to these strain values was constant. The specimen was subjected to 'n' number of fatigue cycles sequentially, without being dismounted from the testing machine and this number go from 10 to 1 million cycles.

In order to do this kind of mechanical test, the testing machine INSTRON E10000 was used; it had 10KN as a load capacity.

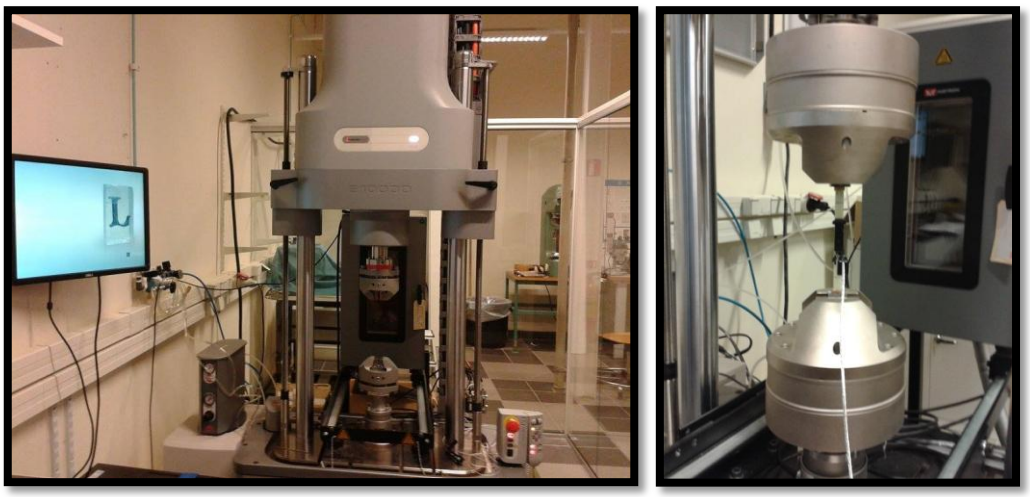

Figure32.The INSTREON machine E 10000

The tested specimens were subjected to the following load ramp containing three steps.
Step 1 and 3 were similar and they were used to do stiffness's measurement. Their maximum strain was 0.25 % when the cycles were done with 0.2% of strain or 0.35% where the strain values during the fatigue cycles were higher than 0.3%. The stiffness of the specimen was calculated before and after 'n' fatigue cycles represented in step 2.

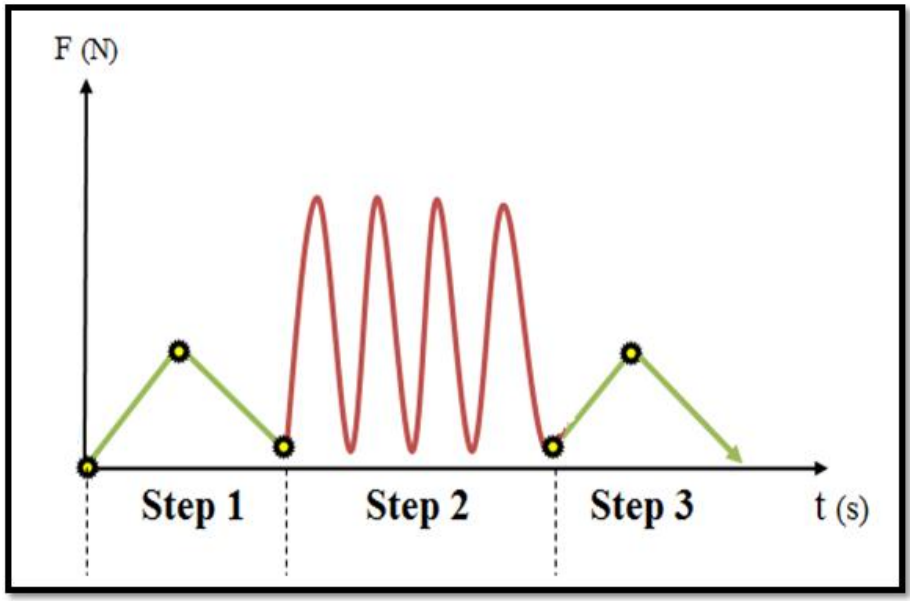

Figure33.Load as a function of time

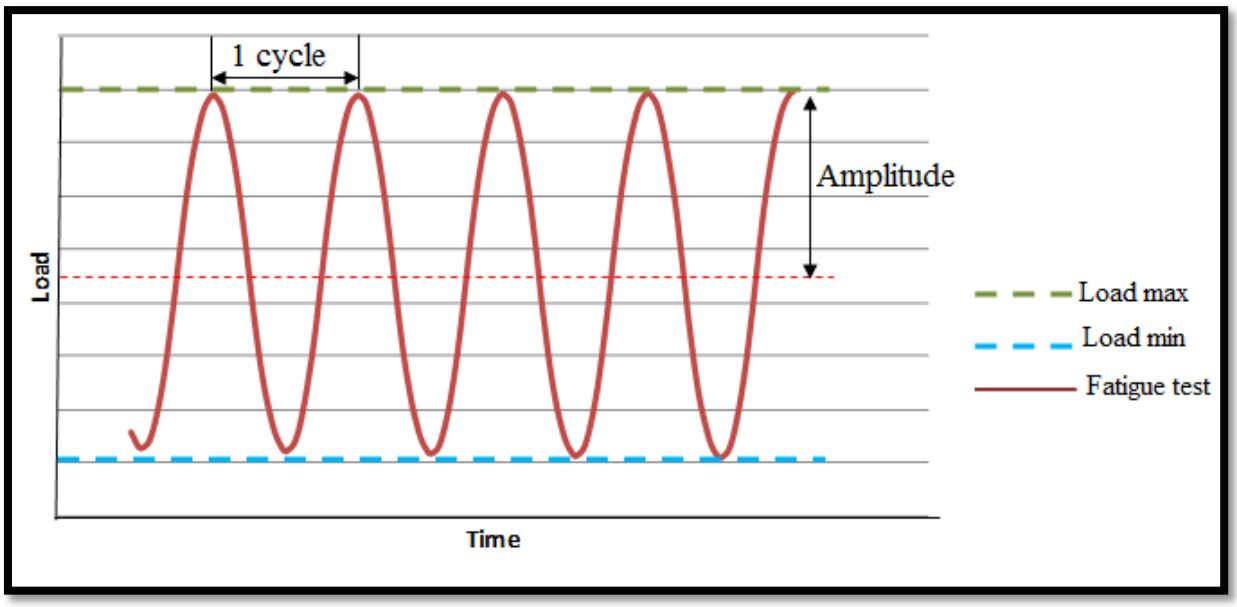

Figure 33.Mechanical fatigue test parameters

The fatigue tests were conducted at stress ratio (R), $\sigma_{min} / \sigma_{max} = 0.1$ at a frequency 5 Hz and with a sinusoidal waveform having an amplitude equal to;

$$\text{Amplitude} = \frac{F_{max} - F_{min}}{2}$$

Such as F_{max} and F_{min} are respectively the maximum and the minimum load reached in the fatigue cycle.

The ramp rate is calculated using the next relation:

$$R_R = (0.01 \times E_0 \times A)/60$$

This ramp rate is expressed in N/s; where E_0 is the initial modulus before the fatigue test and A is the area of the tested specimen.

During this test the specimen wasn't dismounted and after each number of cycles the matrix cracks in the marked area were counted by simple optical observation using the reflected light.

An assumption was done for the fatigue tensile test and it considered that the cyclic loading reduce the resistance of the layer to failure. To adapt the Weibull distribution to this situation it was assumed that the weakest position in the layer regarding crack initiation in quasi-static test is the weakest position also in cyclic loading. Then the Weibull's assumption could be described as following;

$$n(\sigma_T) = f(N) \left(\frac{\sigma_T}{\sigma_0}\right)^m \quad (16)$$

Where $n(\sigma)$ is a function characterizing the number of defects per unit of volume which at stress σ can develop in cracks depends also on the number of cycles (Damage increase with the increasing number of fatigue cycles).

m and σ_0 represent the Weibull's parameters determined in quasi-static test (as it was explained in the previous part of static tensile test).

The simplest form of this function;

$$n(\sigma_T) = N^{\alpha} \left(\frac{\sigma_T}{\sigma_0}\right)^m \quad (17)$$

N is the number of fatigue cycle

Leading to

$$P_f = 1 - \exp\left[-\frac{V}{V_0} N^{\alpha} \left(\frac{\sigma_T}{\sigma_0}\right)^n\right] \quad (18)$$

The double logarithm of the distribution;

$$\mathrm{Ln}(-\ln(1-P_f)) = \alpha \ln N + m \ln \frac{\sigma_T}{\sigma_0} + \ln \frac{V}{V_0} \quad (19)$$

2. Results and discussion

2.1. Strain value during fatigue cycles = 0.4%

In this part three specimens were subjected to the load control test under maximum strain value equal to 0.4 %. The stiffness's measurement after and before performing 411160 cycles were represented in the next table represents:

Specimens (Thickness/width)	Young modulus before n fatigue test (GPa)	Young modulus after n fatigue test (GPa)	Stiffness reduction (%)
1 (2.79/12.19)	19.831	17.515	11.68
2 (2.97/10.83)	19.707	17.900	9.17
3 (2.94/11.28)	18.580	16.601	10.65

Table5. Experimental measurements

'n' was the number of fatigue cycles equal to 411160 cycles.

The initial Young's modulus of three specimens was 10% lower than the modulus value got from the value used to calculate the Weibull's statistic (23 GPa).

The stiffness values for the three specimens were lower after performing the fatigue test, and this was due to the mechanical damages came from the high stress applied during the cycling loading.

The first damage observed in the composite laminate was the matrix crack (de-bonding between fibers and matrix) in the 90°-layer and that as consequence affected the whole stiffness of the cross-ply as it is represented in the figure;

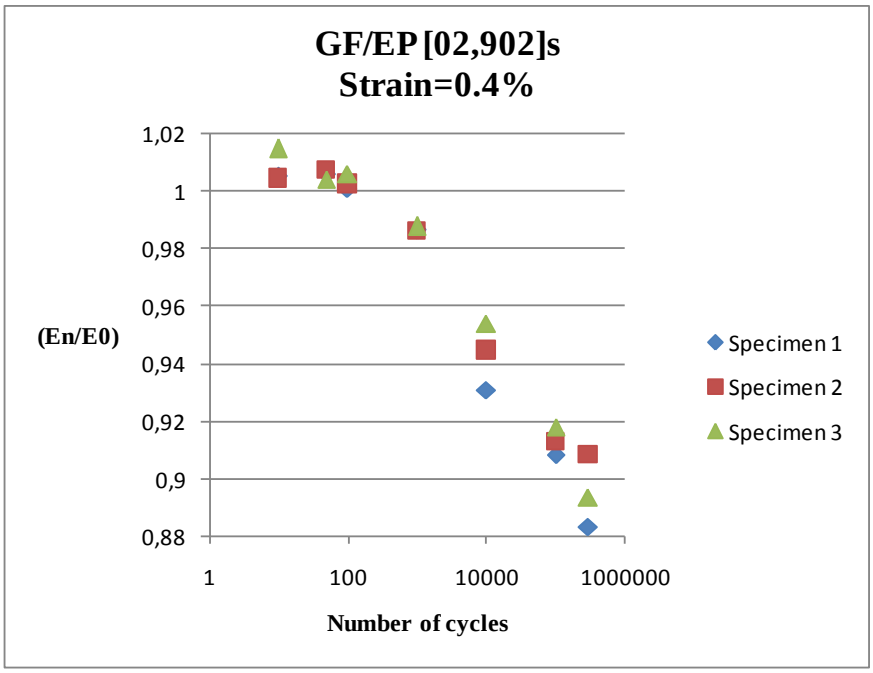

Figure 34.Stiffness reduction as a function of cycle's numbers

As it was shown from the previous curves, the stiffness behaved in the same way for the three specimens; it decreases with the increasing number of fatigue cycles. This was due to the damage accumulation in the specimens. For those specimens, the number of cracks was higher than 20 cracks after performing 10000 cycles and this number increased more during the test as it was represented in the next graph;

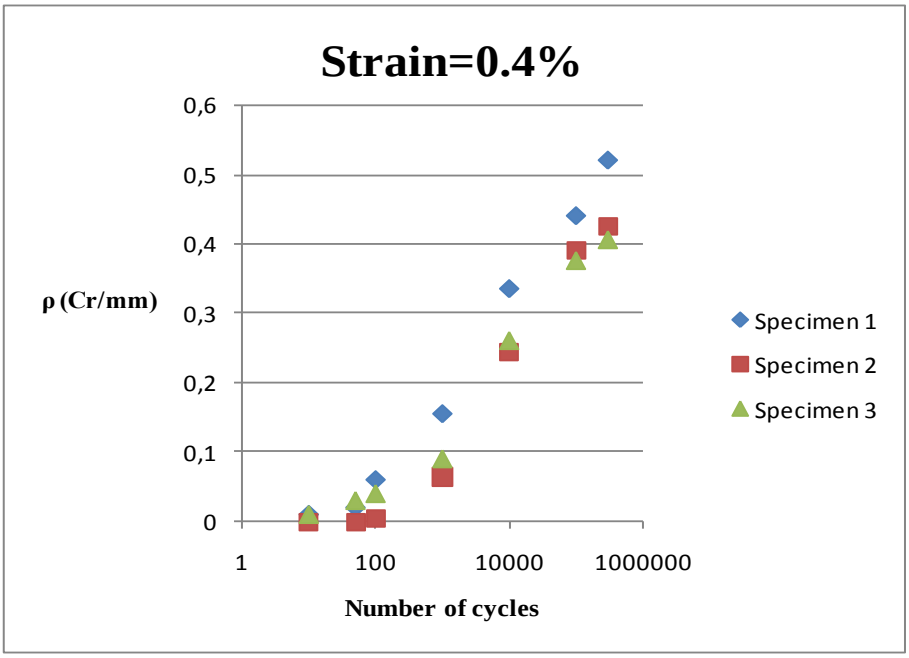

Figure 35.Crack density as a function of number of cycles

2.2. Strain value during fatigue cycles = 0.5% and 0.6%

The same tests were performed for other GE/EP specimens: three specimens were subjected to fatigue cycles with 0.5% of strain and three other with 0.6% of strain. The experimental results describing the stiffness change were represented in the next table and curves;

Strain (%)	Specimens (Thickness(mm))	Young's modulus before n fatigue cycles (GPa)	Young's modulus after n fatigue cycles (GPa)	Stiffness reduction (%)
0.5	1 (2.95)	17.841	15.380	13.79
	2 (2.82)	20.014	17.378	13.17
	3 (2.36)	25.897	22.278	13.97
0.6	1 (2.97)	21.047	17.681	15.99
	2 (2.72)	22.063	19.065	13.59
	3 (2.93)	19.772	17.140	13.31

Table 6.The Young modulus measurement before and after n fatigue cycles

(n = 411160 cycles)

During the manufacturing process, the amount of the resin squeezed out of the plate was different from plate to another, within the same plate the volume of the resin was not uniform and also the volume fraction that why we got specimens with different thicknesses. This geometric grandeur (thickness) influenced, sometimes, the stiffness. As it was shown in this table, the thinner specimen (strain=0.5%, specimen 3) had the greater initial Young's modulus, and this could be explained in case of lack of resin the stiffness of the specimen was defined by the fibers stiffness which was greater than the resin's stiffness.

It was noted from this table, that the stiffness represented a reduction between 13 % and 16%. Those percentages were higher comparing to that got with 0.4% of strain value. The stiffness then was influenced by the strain value. From the next curves it was noted that the normalized stiffness deceased with the increasing number of fatigue cycles. So the stiffness was influenced also by the number of fatigue cycles.

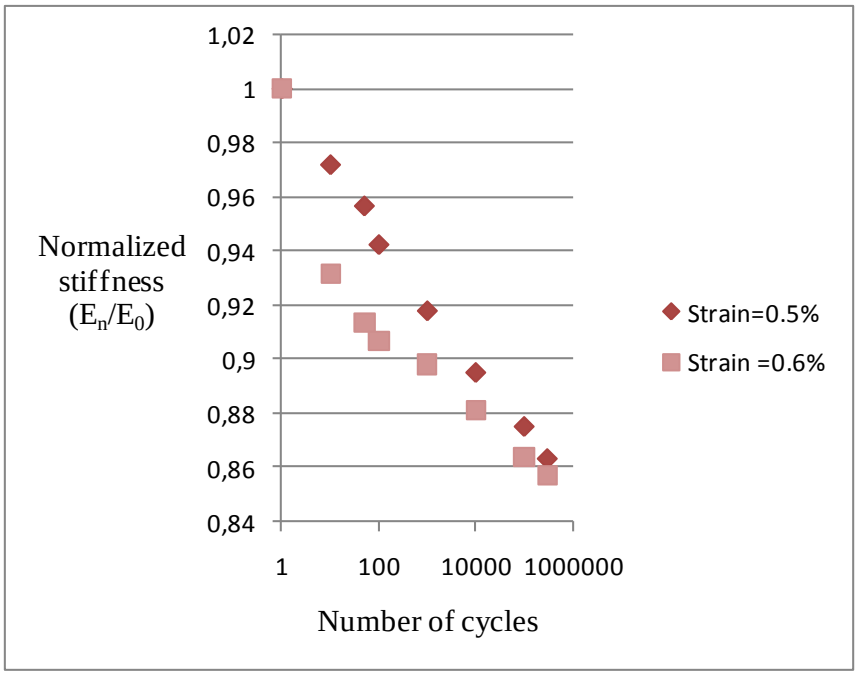

Figure 36.The average normalized stiffness of three specimens as a function of cycle's number

Because of the high stress applied on the specimens during the fatigue tensile test, the damage initiation take place, the matrix cracks began to appear after performing 10 cycles and then it increase during the next cycles. For both strain value, the average crack density was calculated for each three specimen in order to study the evolution of damage as function of number of fatigue cycle

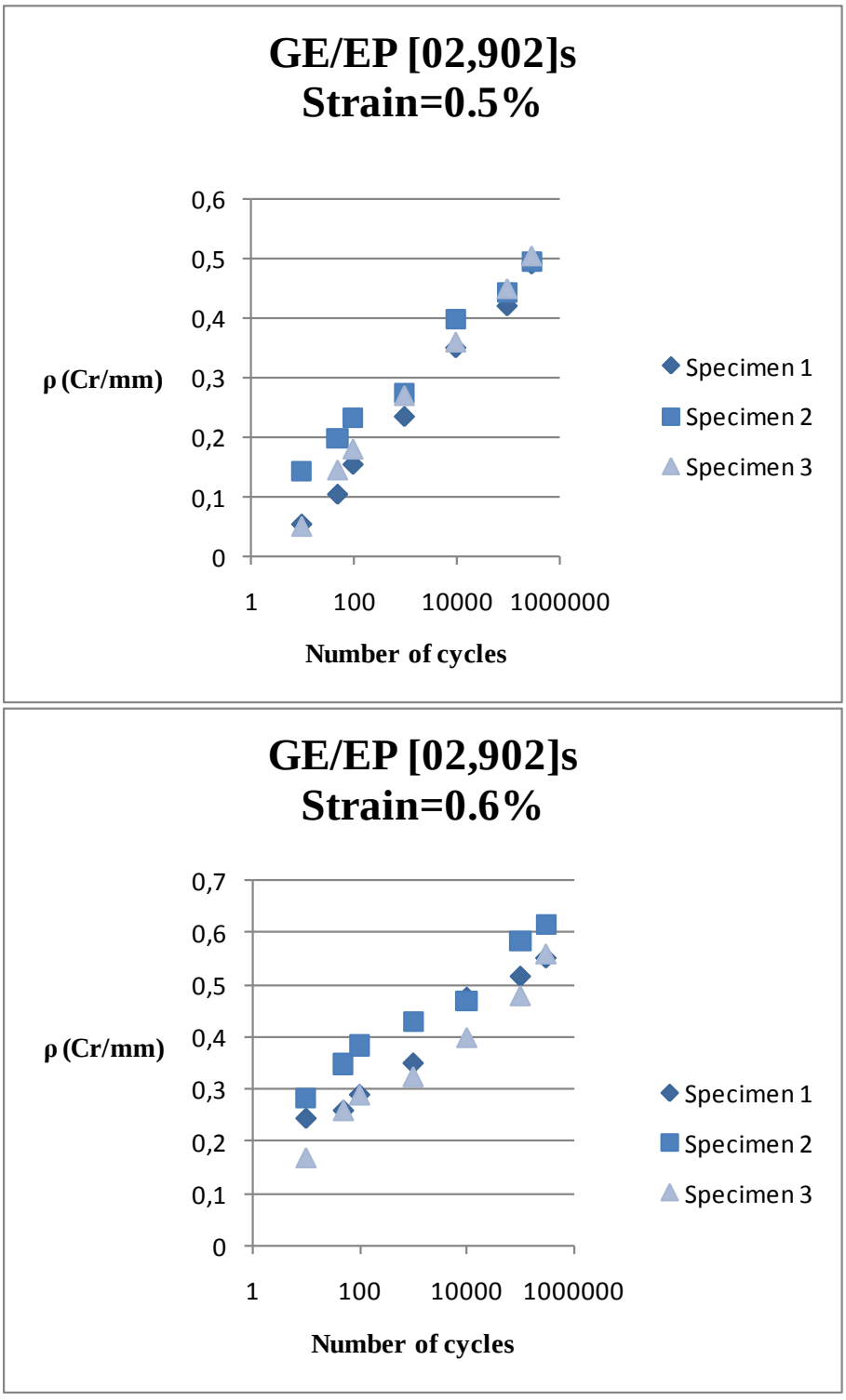

Figure 37.Crack density as a function of number of fatigue cycles for strain value (a) 0.5%. (b) 0.6%.

From this graph, it was noted that the damage evolution increase linearly on log scale with the number of fatigue cycles. And it was also shown that the tests performed with 0.6% of strain value caused more damage in the cross-laminate comparing to the test done with 0.5% of strain value.

2.2.1. Dependency of number of fatigue cycles

In order to study the cycle dependency of cracking, the double logarithm of the Weibull distribution (described in the fatigue tensile test part) versus logarithm of number of cycles curves were plotted for two strain values 0.5% and 0.6% as following;

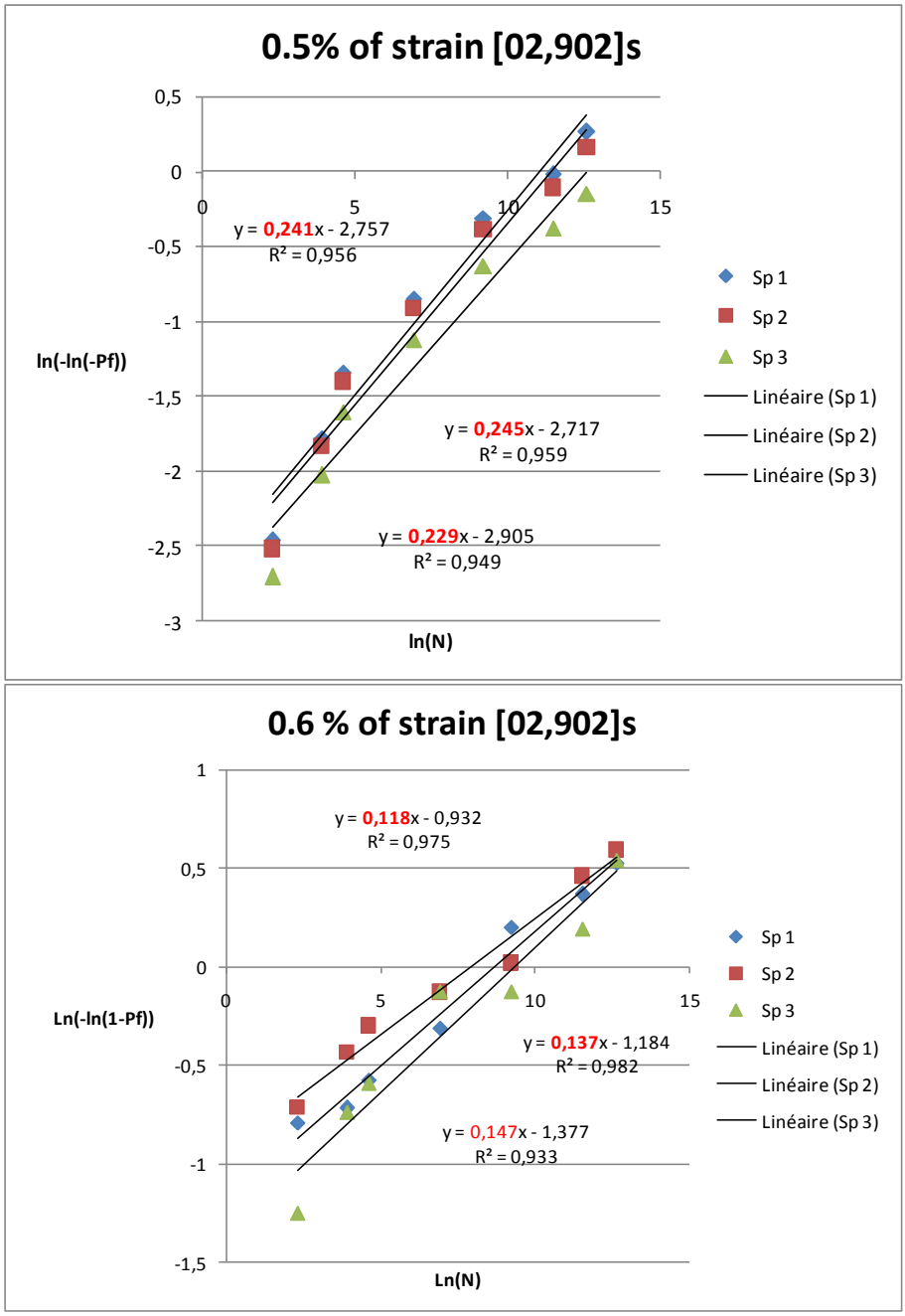

Figure 38. Cycle dependence of cracking a) at 0.5% applied strain; b) at 0.6% applied strain

The slop of those curves represented the values of α. This was the same for 3 specimens subjected to the same strain value, but it had different value from strain 0.5% and 0.6%.

According to the assumption those slops should be approximately equal to each other but as this α was not the same for 0.5% and 0.6% of strain, so it couldn't be considered as material property.

2.3. Strain value during fatigue cycles = 0.7%

One more fatigue cycles done with 0.7% of strain value. Three specimens were subjected to 411160 fatigue cycles. The stiffness measurements were represented as following;

Specimens (Thickness/width)	Young modulus before n fatigue test (GPa)	Young modulus after n fatigue test (GPa)	Stiffness reduction (%)
1 (2.93/10.75)	22.801	20.194	11.43
2 (2.96/11.34)	21.205	17.288	18.47
3 (2.61/9)	22.048	18.550	15.86

Table 7.Experimental results

The stiffness of specimen 2 and 3 had undergone a significant decrease after performing 411160 fatigue cycles. The specimen 2 lost 18.47 % of its initial Young modulus value, this percentage was higher comparing to that got with the other fatigue tensile test done with 0.4%, 0.5% and 0.6% as strain value.

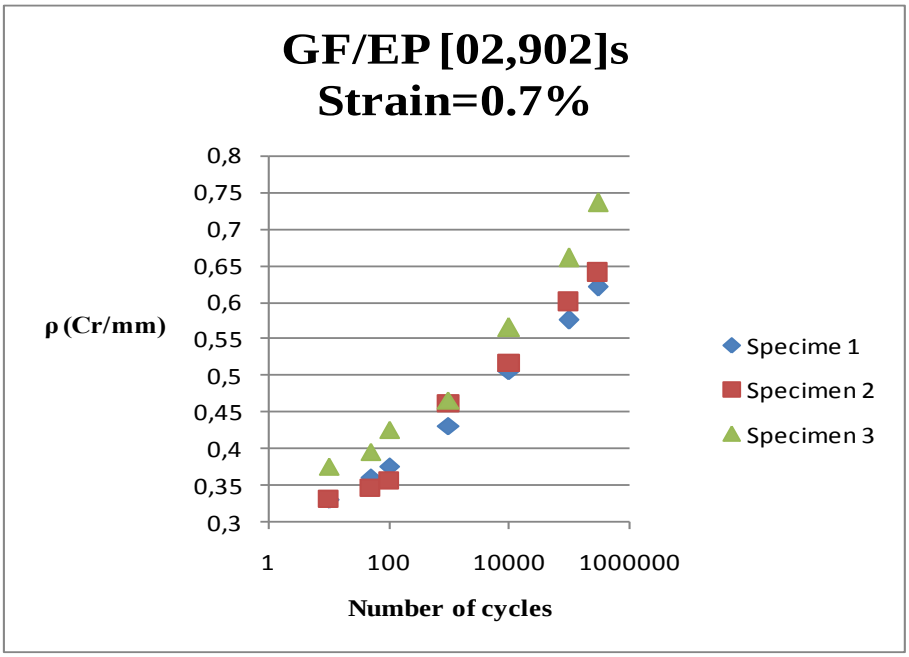

Figure 39.Crack density as a function of number of cycles

Even, after performing only the first 10 fatigue cycles, for the three specimens the crack density was higher than 0.3 Cr/mm. For specimen 3 for example, after performing 411160 cycles the CD was higher than 0.7 Cr/mm.

In addition to the matrix cracks, some delaminations were observed after performing 10000 cycles.

2.3.1. Microscope observation

For the specimens subjected to this test with 0.7% of strain value three damages modes were observed in the 90°-layer:

- Matrix crack: The first damage mode appears after performing the first 10 cycles.
- Delamination: The second damage mode appears after performing 10000 fatigue cycles, and it length increased with the increasing number of cycles.
- Longitudinal cracks: The third damage mode appeared after performing 100.000 fatigue cycles.

An optical microscope observation was done in order to see the damage modes already cited:

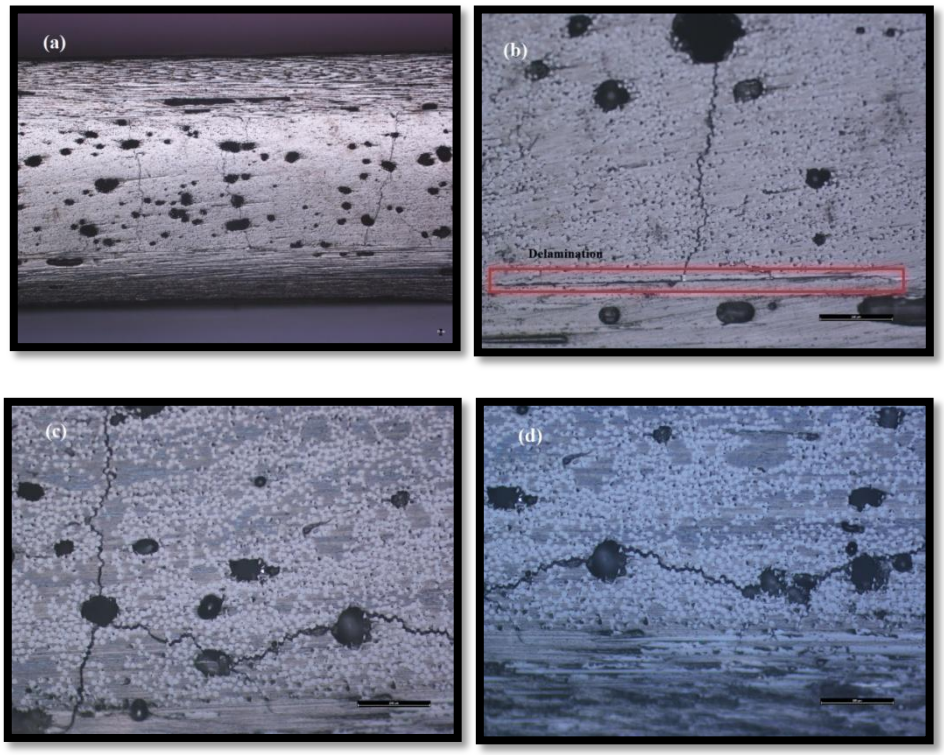

Figure 40. (a) Microscope observation of tested edge (scale 10µm). (b) Delamination (scale 200 µm). (c) and (d) Longitudinal crack in layer 90°(scale 200 µm)

After taking those pictures, the specimen was polished again in order to check if the longitudinal cracks were just an edge effect or not. For that the specimen was polished down and 0.5 mm were removed. The result was that those cracks remain in the 90°-layer even after polishing as it is represented in the next picture;

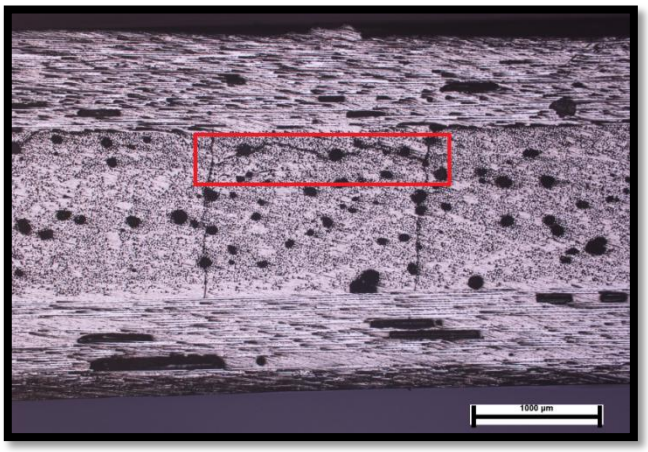

Figure 41.Microscope observation of cracks after polishing

2.4. Results comparison

In this part a comparison of damages evolution was done, the CD versus strain curves were plotted after performing 100000 and 411160 fatigue cycles. Each point in the following curves represents the average of crack density of 3 tested specimens;

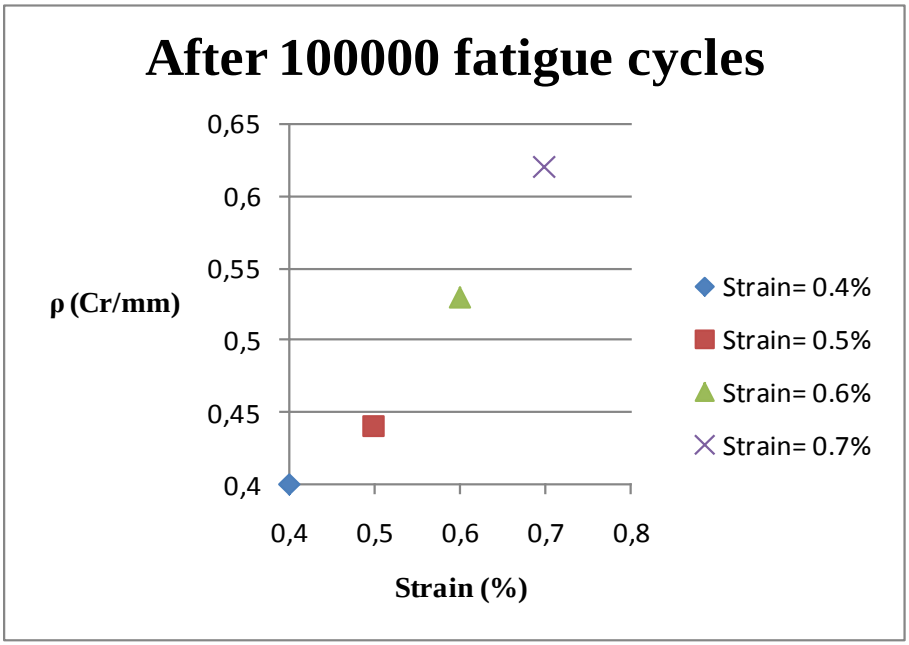

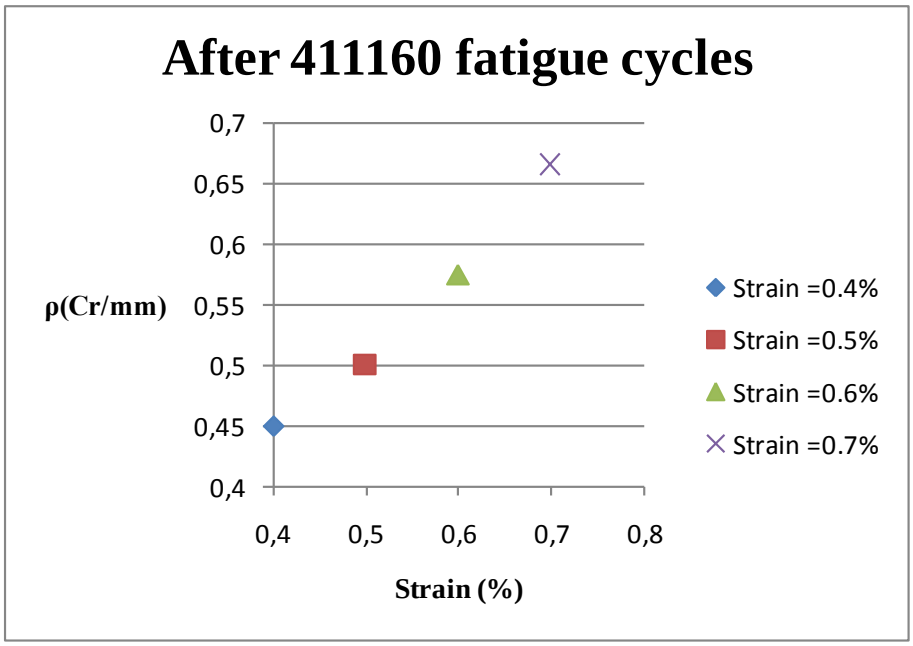

Figure 42.Crack density versus strain (a) After 100000 fatigue cycles, (b) After 411160 fatigue cycles

From the two graphs it was shown that there was no big difference between the crack density got from 0.4% and 0.5% of strain value. The highest crack density was shown at 0.7% of strain (matrix cracks, delamination and longitudinal cracks are shown). After performing 411160 fatigue cycles, the CD values were higher than that obtained after performing 100000 fatigue cycles.

Chapter 6:

Fatigue tensile test followed by quasi-static tensile test

1. Methodology

In this final part, the specimens were subjected to two mechanical tests, the fatigue tensile test followed by the quasi-static tensile test. The tests were done using the same INSTRON machine. The same measurements (stiffness and crack density evolution) as previously were done.

The total number of fatigue cycles was 1100000 for the specimens tested with 02% of strain value, and it is 1101100 for those tested with 0.3% of strain.

2. Result and discussion

2.1.Strain during the fatigue test = 0.2%

The tested specimens have the following geometry;

Specimens	Initial elastic modulus (GPa)	Thickness (mm)	Width (mm)
1	19.99	3	11.66
2	20.56	3.02	11.07

Table 8. Thickness and width of 2 specimens

After performing 1100000 fatigue cycles, there was no modulus reduction (~ 0%) and the maximum CD reached was 0.07 Cr/mm which was very low comparing to the number of cracks got in the previous tests (0.4%,0.5%,0.6% and 0.7%).

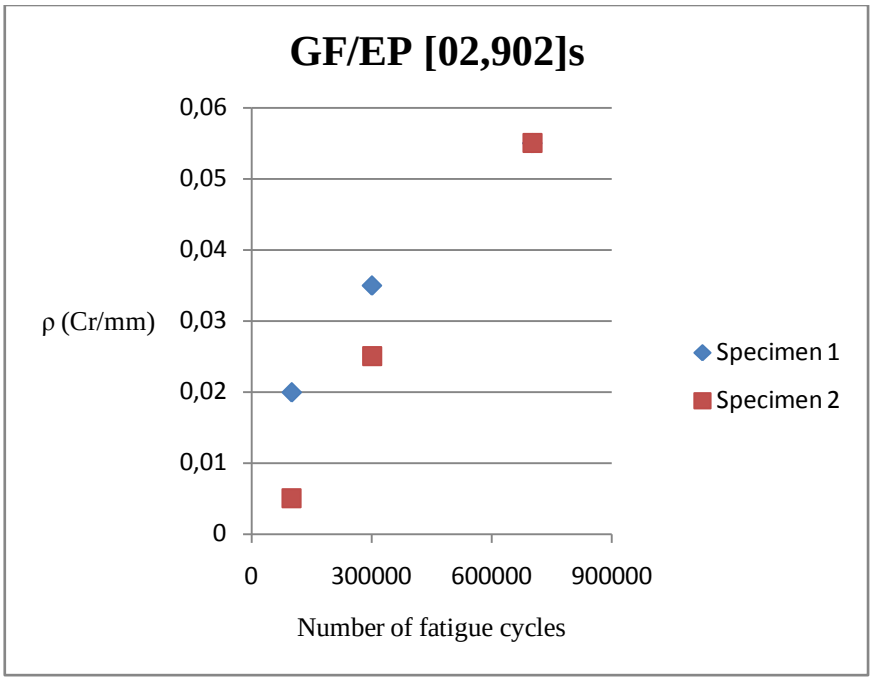

Figure 43. Crack density evolution as function of number of cycles

From this graph (figure 41) it was noted that there were some damages after performing the fatigue cycles. Those cracks continue their evolution during the quasi-static test as it is represented in the following graphs;

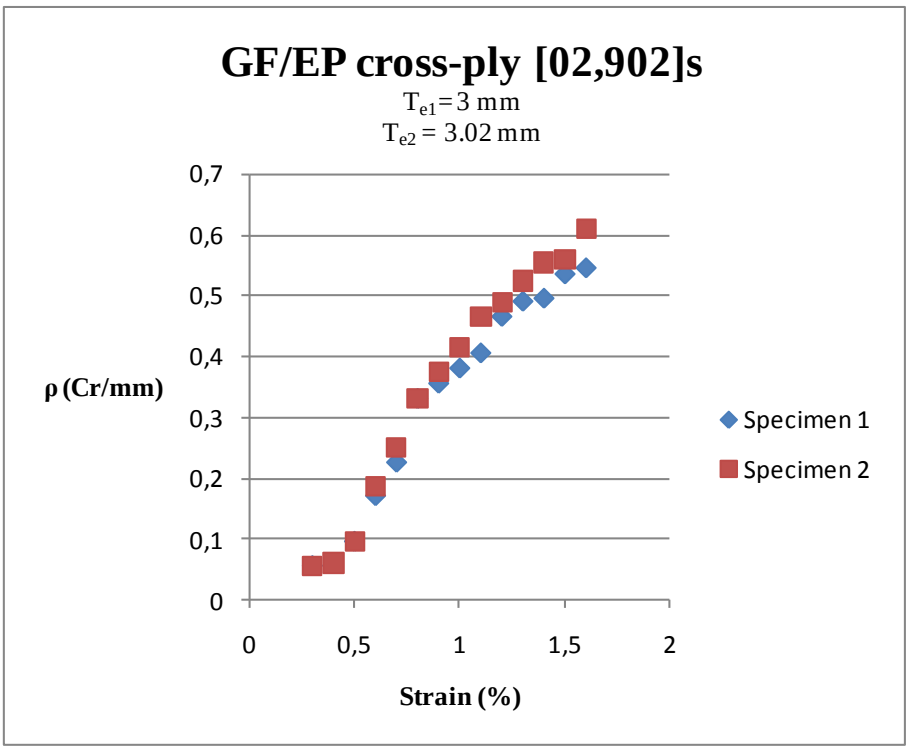

Figure 44. Crack density as function of strain in quasi-static loading

2.1.1. *Weibull's statistic*

After performing the static tensile test, the two curves P_f versus σ_T and the double logarithm of the statistic distribution versus the logarithm of σ_T were plotted in order to get the Weibull's parameters;

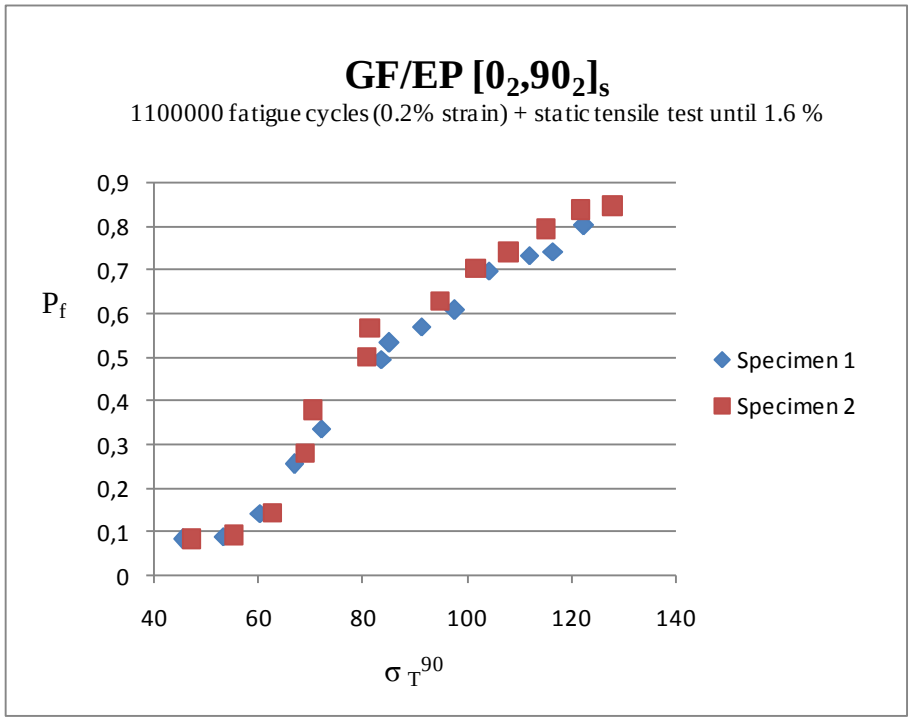

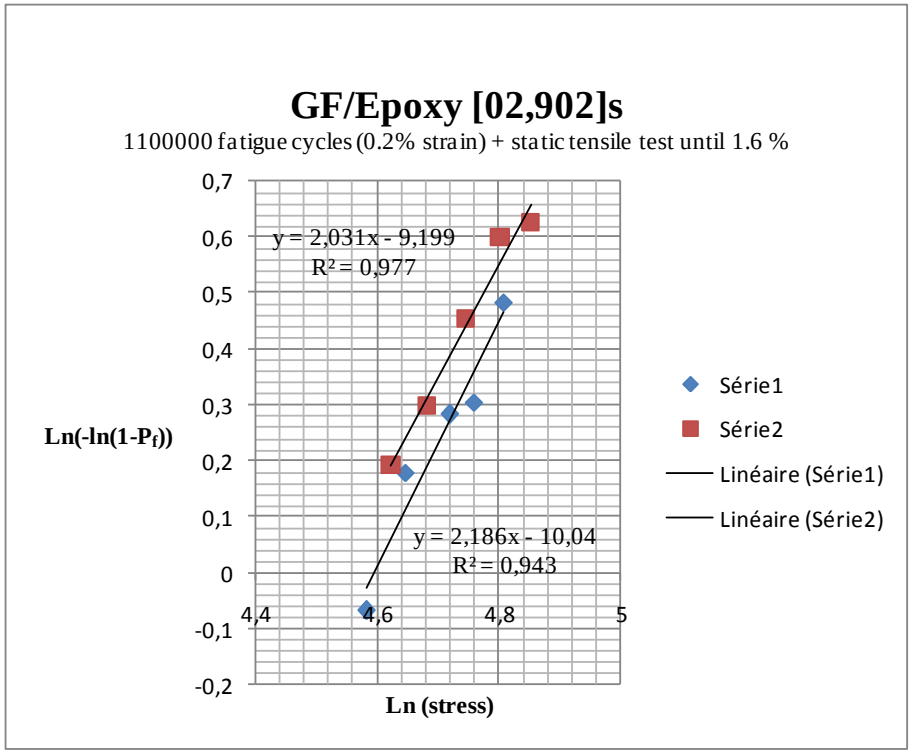

Figur 45.(a) Probability of intra-laminar cracking in 90° layer as a function of thermo-mechanical transverse stress. (b) Ln(-ln(1-P_f)) versus Ln (stress)

These two graphs were plotted using the data starting from 1% strain value in order to do a comparison later with the curves plotted with 0.3% of strain. According to figure 45 the shape and scale Weibull's parameters for the two tested specimens were obtained;

$n_1 = 2.031$	$\sigma_{01} = 92.69$ MPa
$n_2 = 2.186$	$\sigma_{02} = 98.77$ MPa

The average stresses of those two specimens were calculated:

$$\overline{\sigma}_1 = 82.126 \text{ MPa} \quad \text{and} \quad \overline{\sigma}_2 = 87.47 \text{ MPa}$$

2.2. Strain during the fatigue test = 0.3%

Two other specimens were subjected to the same test combination with 0.3% of strain during the fatigue cycles. The tested specimens had the following geometry;

Specimens	Initial elastic modulus (GPa)	Thickness (mm)	Width (mm)
1	18.58	2.67	9.13
2	22.04	2.67	9.10

Table 9. Thickness and width of 2 specimens

After performing 1101100 fatigue cycles, the modulus reduction was equal to 18.20% and 8.25% respectively to the specimens 1 and 2. The maximum CD reached was 0.55 Cr/mm. The crack density versus the number of cycles is represented as following;

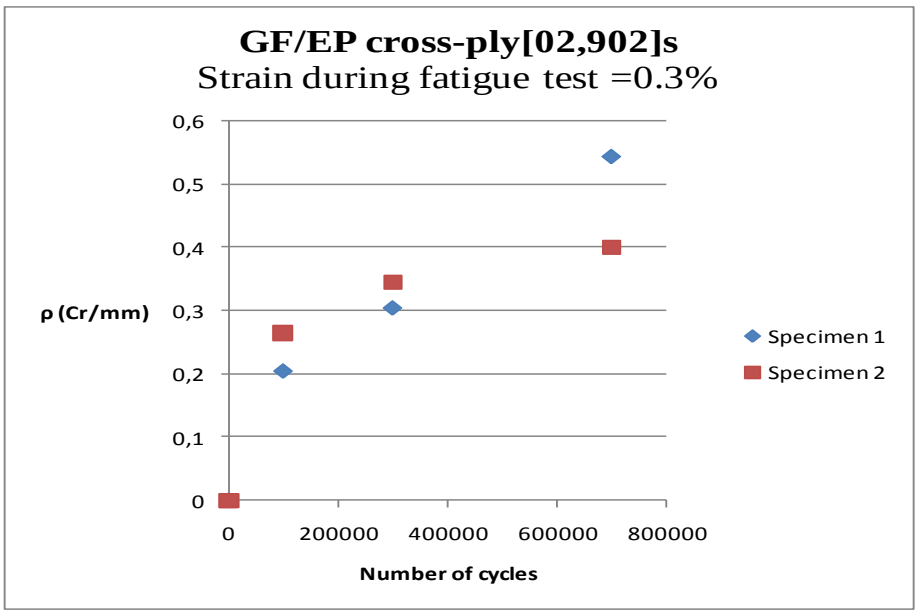

Figure 46. Crack density as a function of number of cycles

These crack densities increased more after performing the static tensile test;

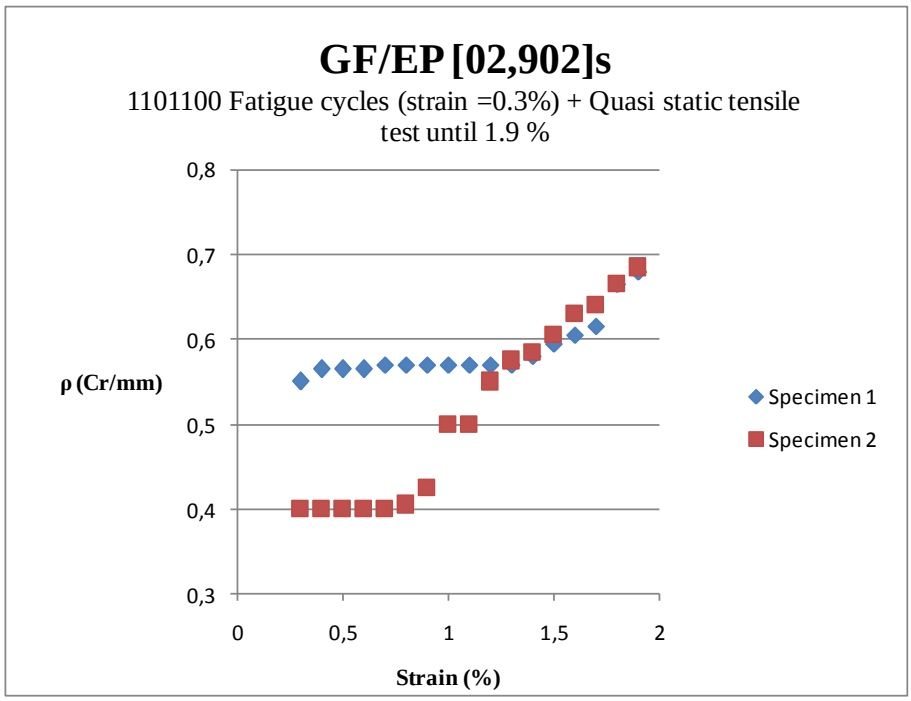

Figure 47. Crack density as a function of strain

It was shown in the figure 45 that until a certain strain level (approximately 1.3%) the crack density still approximately constant for the two specimens. The number the cracks still the same as that obtained after performing the fatigue test. In this case it could be assumed that the applied stresses were not high enough for creating new cracks. So initiation toke place when the applied stresses were high enough.

2.2.1. Weibull's statistic

In this part, the Weibull's parameters were obtained for two tested specimens as following;

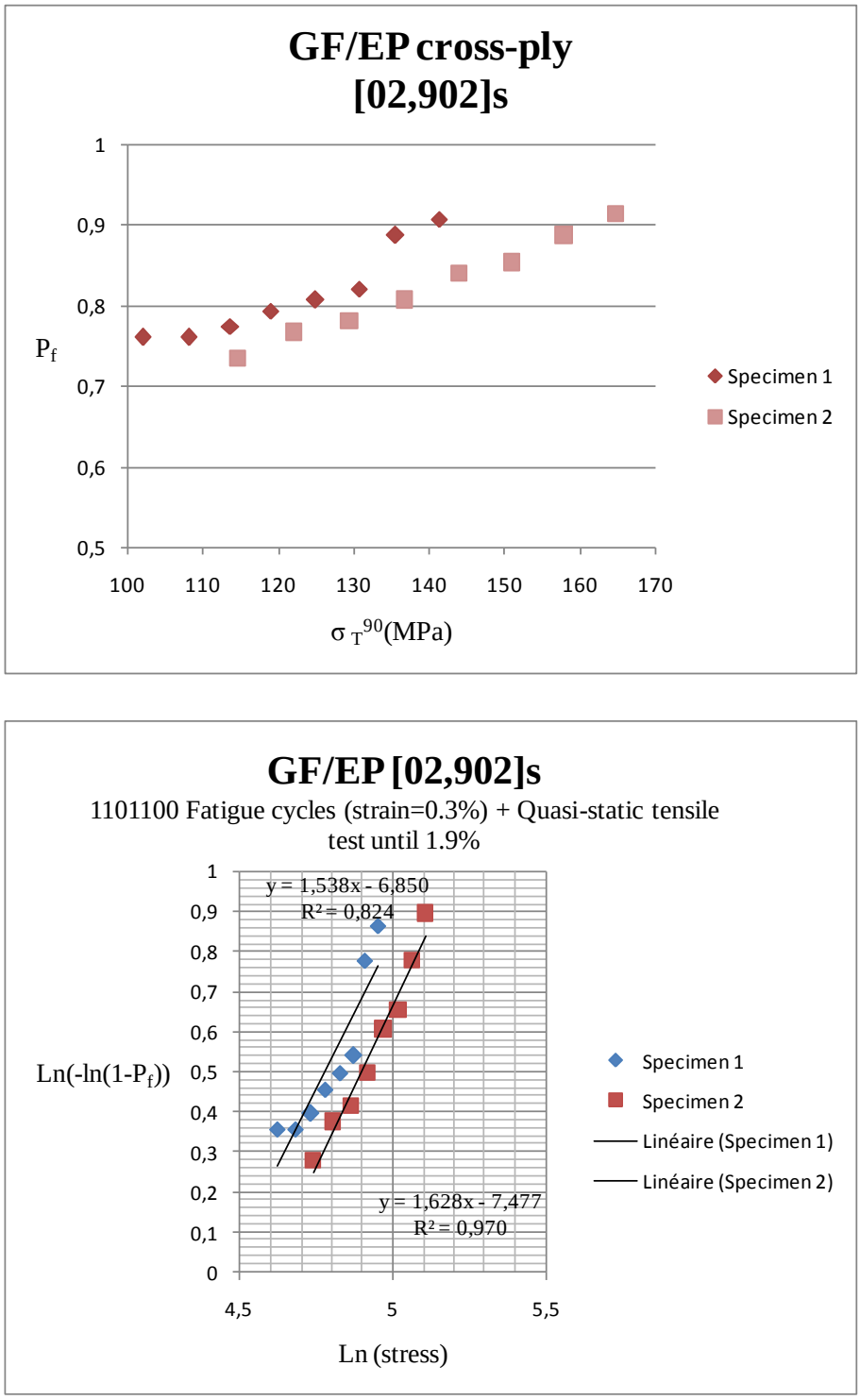

Figur 48.(a) Probability of intra-laminar cracking in 90° layer as a function of thermo-mechanical transverse stress. (b) Ln(-ln(1-P_f)) versus Ln (stress)

These two curves were potted without taking in consideration the horizontal part in figure 47. According to this two graphs the obtained shape and scale Weibull's parameters for the two tested specimens are;

$n_1 = 1.538$	$\sigma_{01} = 85.95$ MPa
$n_2 = 1.628$	$\sigma_{02} = 98.76$ MPa

The average stresses of those two specimens were obtained:

$$\overline{\sigma_1} = 77.37 \text{ MPa} \quad \text{and} \quad \overline{\sigma_2} = 88.41 \text{ MPa}$$

We noted that the average stresses for the specimens subjected to a test combination were lower than the average stresses for the specimens subjected only to a quasi-static test.

Conclusion

In the context of understanding of micro-damage initiation and evolution in GF/EP cross-ply $[0_2,902]_s$ laminates some conclusion were done:

- ✓ The voids percentage and the volume fraction affect the stiffness
- ✓ The first damage mode was the matrix cracks, those cracks appeared in the 90-layer where the fibers direction was perpendicular to the load direction. The transverse properties of layers were lower than the longitudinal properties.
- ✓ After performing any mechanical test, quasi-static test or/and fatigue tensile test there were a stiffness reduction. This mechanical property was affected by the strain value, cracks densities and the number of fatigue cycles.
- ✓ The average transverse strength obtained after performing quasi-static tensile test were higher than the average transverse strength obtained after performing a test combination (quasi-static and fatigue test).
- ✓ The damage increase linearly with the strain value and the number of cycles

References

[1]: F.C. Campbell .Introduction to Composite Materials. Structural Composite Materials.

[2]: Frederick T. Wallenberger, James C. Watson, and Hong Li, PPG Industries, Inc. Glass fibers. 2001 ASM International. All Rights Reserved. ASM Handbook, Vol. 21: Composites.

[3]: P.K. Mallick. Fiber-Reinforced Composites: Materials, Manufacturing, and Design, Third Edition.

[4]: David Hartman, Mark E. Greenwood, and David M.Technical paper titled High strength glass fibers. Lipscomb University. Pub. No. LIT-2006-111 R2 (02/06)

[5]: Manoj Singla and Vikas Chawla.Mechanical Properties of Epoxy Resin – Fly Ash Composite. Journal of Minerals & Materials Characterization & Engineering, Vol. 9, No.3, pp.199-210, 2010.

[6]: R. Bruce .AN INTRODUCTION TO THERMOSETS.Prime IBM (Retired).

[7]: Nicolae ţăranu, raluca hohan and liliana bejan. Buletinul institutului politehnic din iaşi. Longitudinal stiffness characteristics of unidirectional fibre reinforced polymeric composites subjected to tension.

[8]: Ben Khala Hiba. Models for bending stiffness in laminates with intralaminar and interlaminar damage.LTU master thesis.

[9]: Wacker silanes for coatings applications. Industrial coatings / silanes.

[10]: Seth Binfield, Dr. Craig Hillman, Thomas Johnston, and Dr. Nathan Blattau..Conductive Anodic Filaments: The Role of Epoxy-Glass Adhesion.

[11]: Mechanical properties of glass fiber composites with an epoxy resin modified by a liquid crystalline epoxy. Polymer composite book.

[12]: Christian Heinrich and Anthony M. Waas† University of Michigan, Ann Arbor, Investigation of progressive damage and fracture in laminated composites using the smeared crack approach. Michigan, 48109, USA.

[13]: S T Pinho , P Robinson , L Iannucci .Fracture toughness of the tensile and compressive fibre failure modes in laminated composites..

[14]: Janis Varna .Book titled Damage evolution modelling in laminates.LTU.

[15]: Yongxin Huang. Damage Evolution in Laminates with Manufacturing Defects.. LICENTIATE THESIS in LTU.

[16]: J.A.M. Ferreira a, J.D.M. Costa , P.N.B. Reis b, M.O.W. Richardson .Analysis of fatigue and damage in glass-fibre-reinforced polypropylene composite materials.Composites Science and Technology 59 (1999) 1461±1467.

[17]: Mohammed A Torabizadeh. Tensile, compressive and shear properties of unidirectional glass/epoxy composites subjected to mechanical loading and low temperature services.
Indian journal of engineering and materials science. Vol 20, August 2013, pp. 299-309.

[18]: S. SPRENGER, A.C. TAYLOR, A.J. KINLOCH, C.M. MANJUNATHA. The Tensile Fatigue Behaviour of a Glass Fiber Reinforced Plastic Composite Using Hybrid Toughened Epoxy MatrixJournal of Composite Materials, vol. 44, 2010, 2095-2109.

[19]: Robert Joffe. Damage accumulation and stiffness degradation in composite laminates. LTU Doctoral thesis.

[20]: Peter Lundmark. Damage mechanics analysis of inelastic behavior of fiber composites.. LTU DOCTORAL TH E S I S.

[21]: H.Ben khala and J.Varna and A.Purpus. Microcracking in layers of composite laminates in cyclic loading with tensile transverse stress component in layers.LTU